Coronal loop seismology

using damping of standing kink oscillations by mode coupling

D.J. Pascoe
C.R. Goddard, G. Nisticò, S. Anfinogentov, V.M. Nakariakov

Centre for Fusion, Space and Astrophysics
University of Warwick, Coventry, UK

SolarNet 5 Workshop
Queen's University Belfast
1 September 2016

Overview

- Introduction (damped kink oscillations of coronal loops)
- Mode coupling by resonant absorption as damping mechanism
- Gaussian damping regime
  - numerical simulations
  - analytical theory
  - observational evidence
- Use of both exponential and Gaussian damping regimes for loop seismology
  - application to SDO/AIA observations
- Implications for heating

Standing kink modes of coronal loops

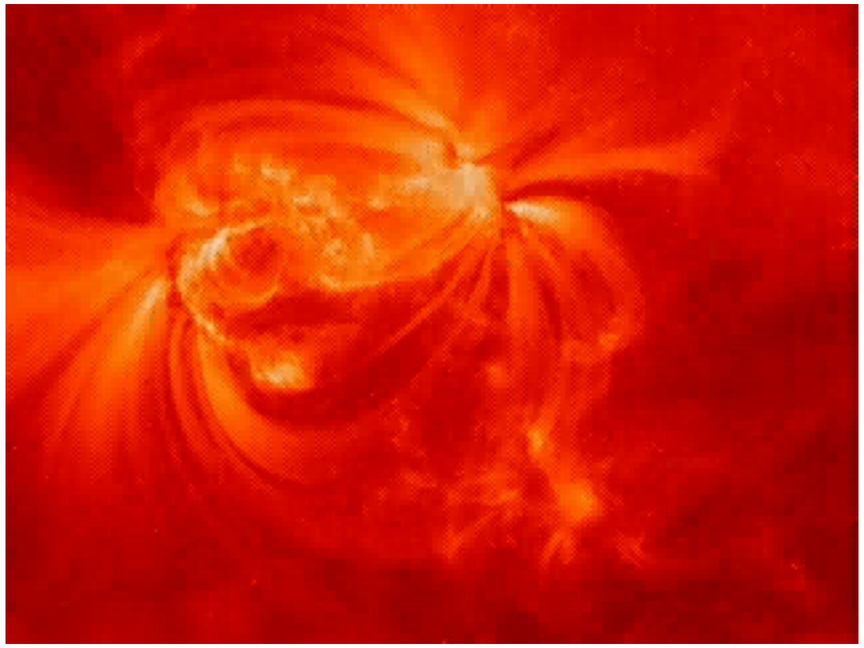

TRACE observation 14 July 1998

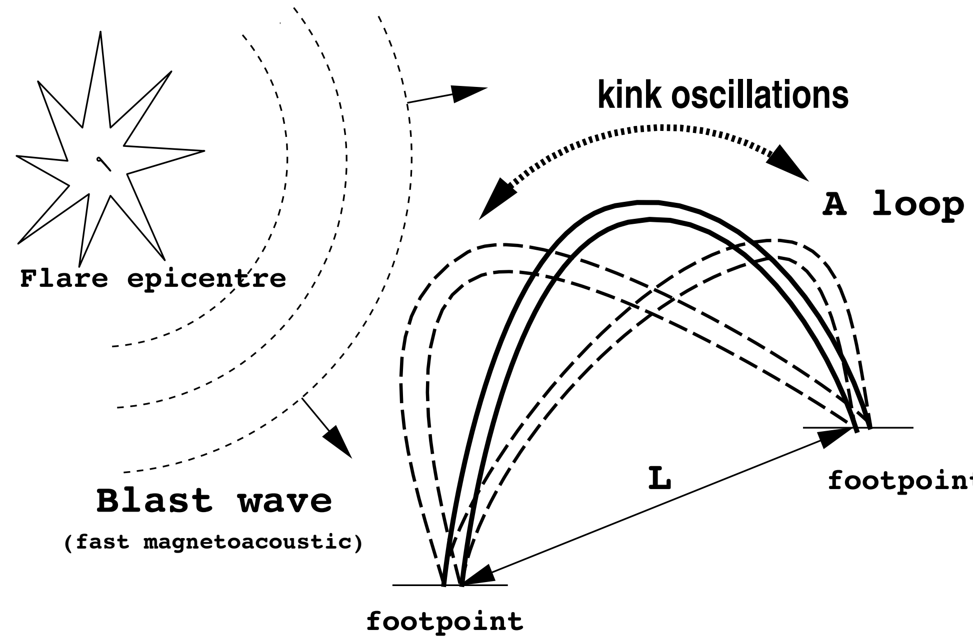

$$\frac{\omega}{k} = \frac{2L}{P} \approx \begin{cases} 1020 \pm 132\ \mathrm{km\,s^{-1}}\ \text{(14th July, 1998)}, \\ 1030 \pm 410\ \mathrm{km\,s^{-1}}\ \text{(4th July, 1999)}. \end{cases}$$

$$k = \pi/L$$

long wavelength limit: $ka \ll 1$

slow $\quad \dfrac{\omega}{k} \approx C_{\mathrm{T0}} \equiv \dfrac{C_{\mathrm{s0}} C_{\mathrm{A0}}}{(C_{\mathrm{s0}}^2 + C_{\mathrm{A0}}^2)^{1/2}}$

$\dfrac{\omega}{k} \approx C_{\mathrm{k}} \equiv \left(\dfrac{2}{1 + \rho_{\mathrm{e}}/\rho_0} \right)^{1/2} C_{\mathrm{A0}} \quad$ fast

$$B_0 = (4\pi\rho_0)^{1/2} C_{\mathrm{A0}} = \frac{\sqrt{2}\,\pi^{3/2} L}{P} \sqrt{\rho_0 (1 + \rho_{\mathrm{e}}/\rho_0)}$$

$$B = 13 \pm 9\mathrm{G}$$

Nakariakov & Ofman (2001)

Kink oscillations excited by coronal mass ejections (CMEs)

- Kink mode = transverse oscillation of loop
- 76% of oscillations associated with CMEs observed in white light emission
- 98% accompanied by lower coronal eruptions

Model of Zimovets & Nakariakov (2015)

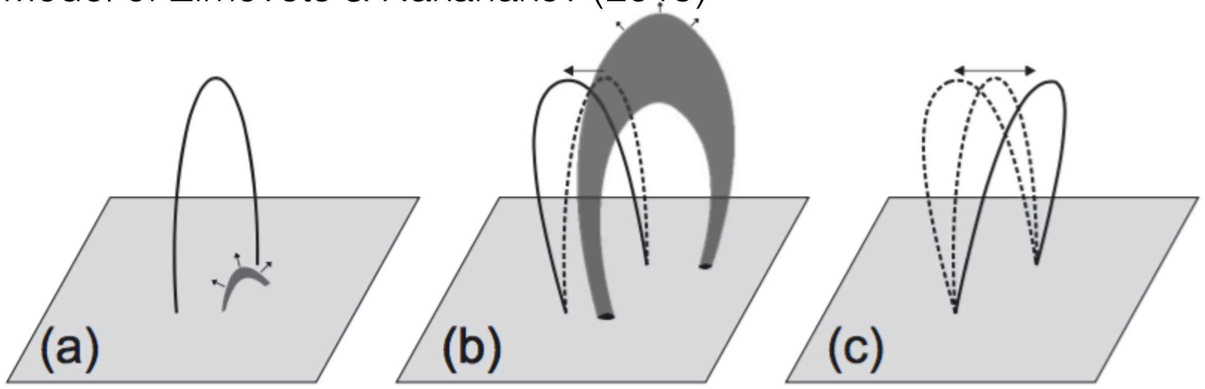

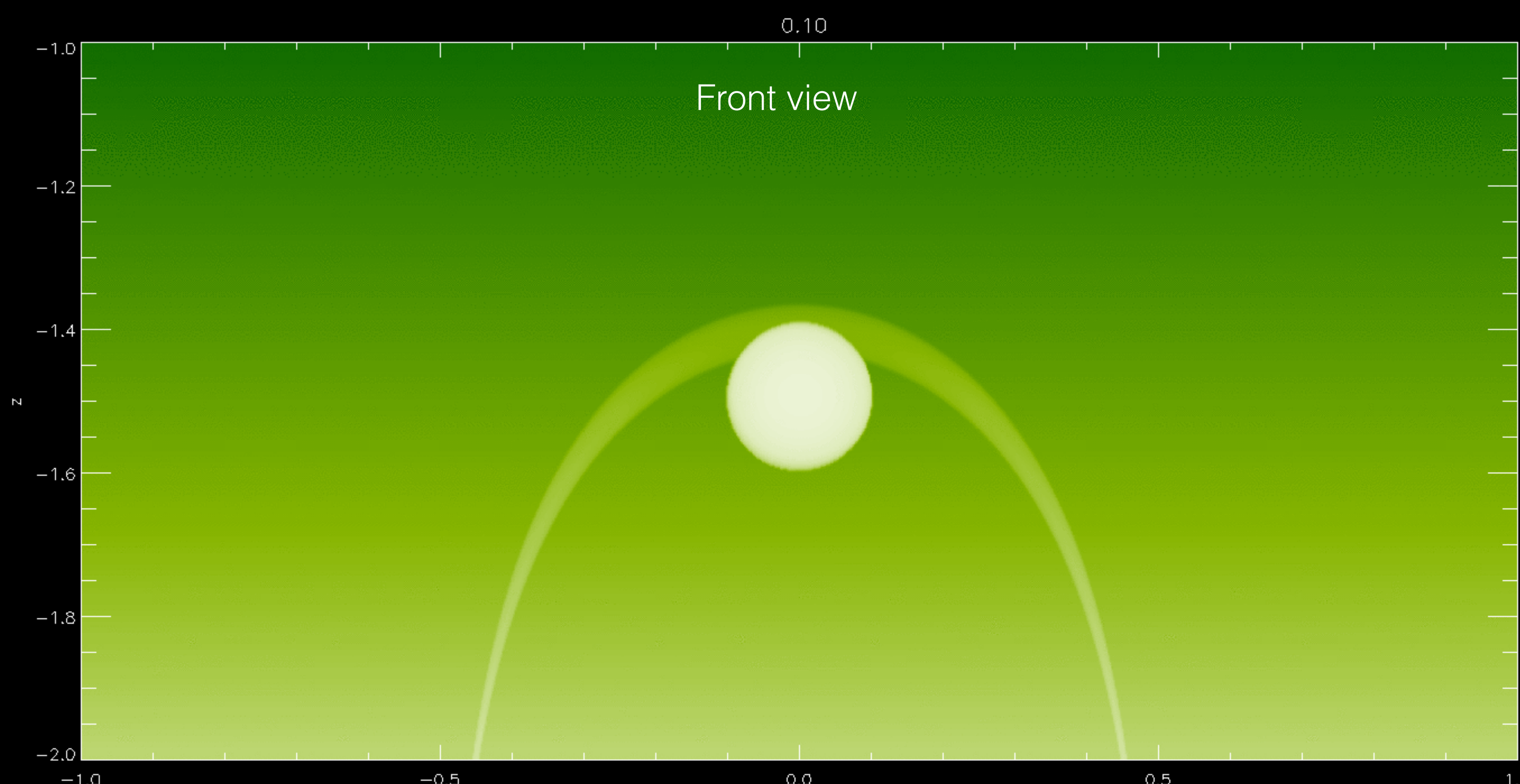

3D simulation by Pascoe & Nakariakov

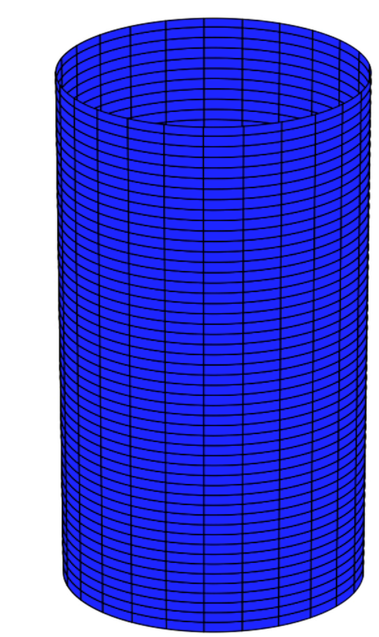

Fundamental kink standing mode

Resonant absorption as a damping mechanism

- Mode coupling studied by Hollweg & Yang (1988), Goossens et al. (1992) etc.
- Ruderman & Roberts (2002) considered in the context of the rapid damping of coronal loop oscillations observed by TRACE
- Modelled damping of kink modes is due to resonant absorption, acting in the inhomogeneous regions of the tube

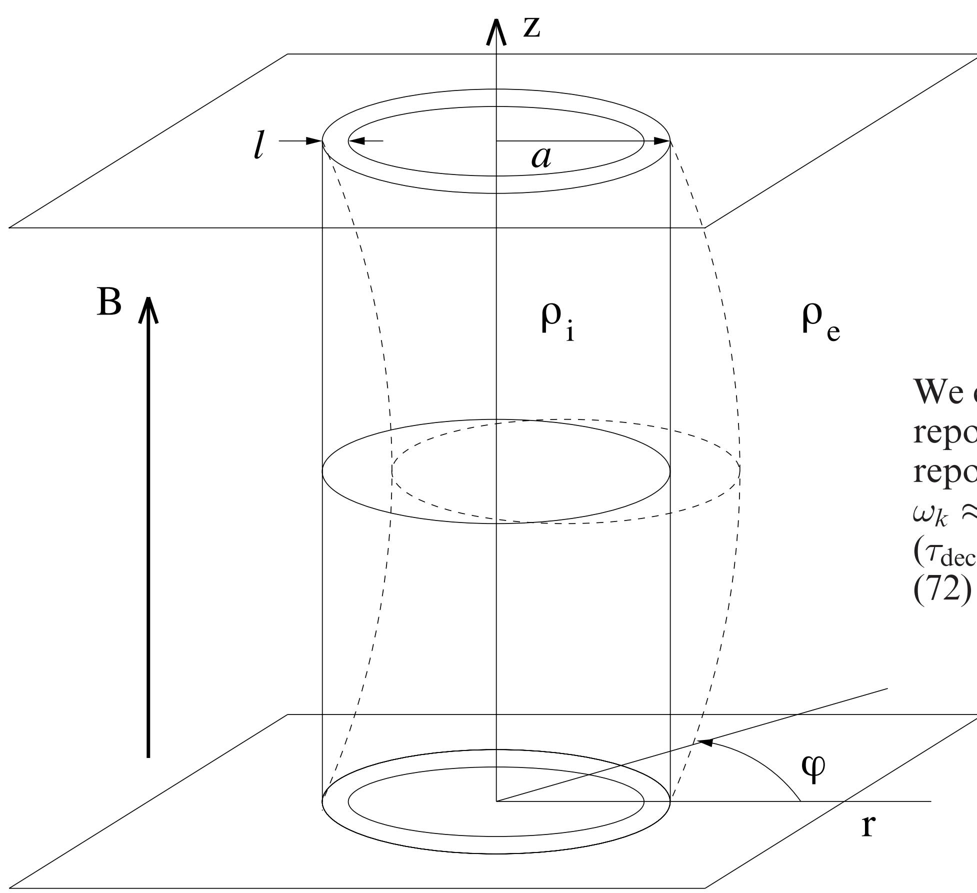

Exponentially damped oscillation with

$$\tau_{\text{decay}} = \frac{2}{\pi}\frac{a}{\ell}\frac{\rho_i + \rho_e}{\rho_i - \rho_e}\tau$$

We consider this result in relation to the observational data reported by Nakariakov et al. (1999). These authors reported a coronal loop oscillation with frequency $\omega_k \approx 0.024\ \text{s}^{-1}$ ($\tau = 256$ s) and decrement $\gamma \approx 0.0011\ \text{s}^{-1}$ ($\tau_{\text{decay}} = 870$ s). Taking $\rho_i = 10\rho_e$, we obtain from equation (72) that $\ell/a \approx 0.23$.

- Transfer of energy from kink mode to Alfvén (azimuthal) oscillations within inhomogeneous layer
- Only loops with small inhomogeneous layers are able to support coherent oscillations

Ubiquitous propagating kink waves

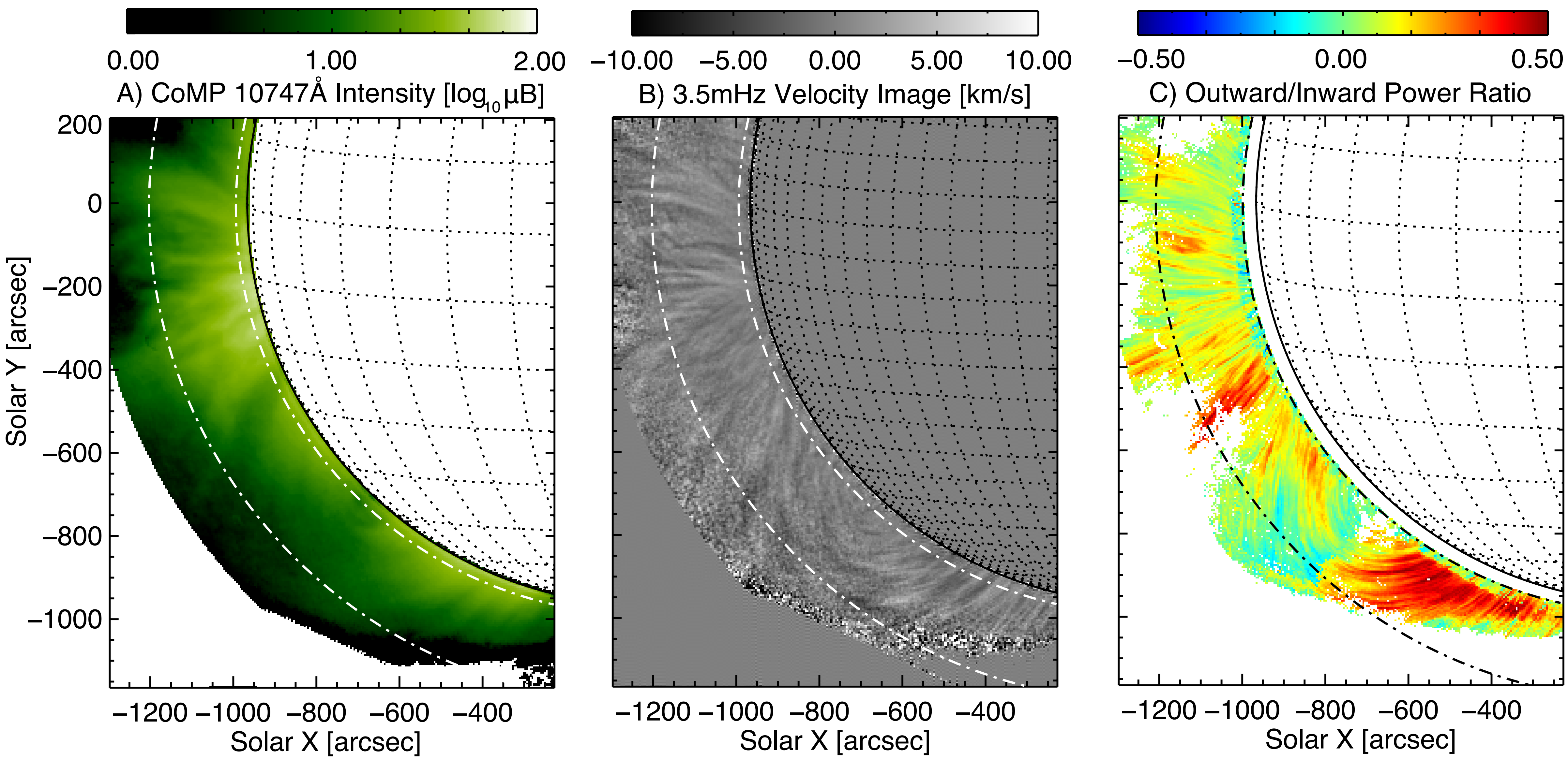

- Ubiquitous transverse velocity perturbations propagating along field lines
- Broadband power spectrum centred on 5 minutes
- Strongly damped

Tomczyk et al. (2007)
Tomczyk & McIntosh (2009)

Wave energy being localised by resonance

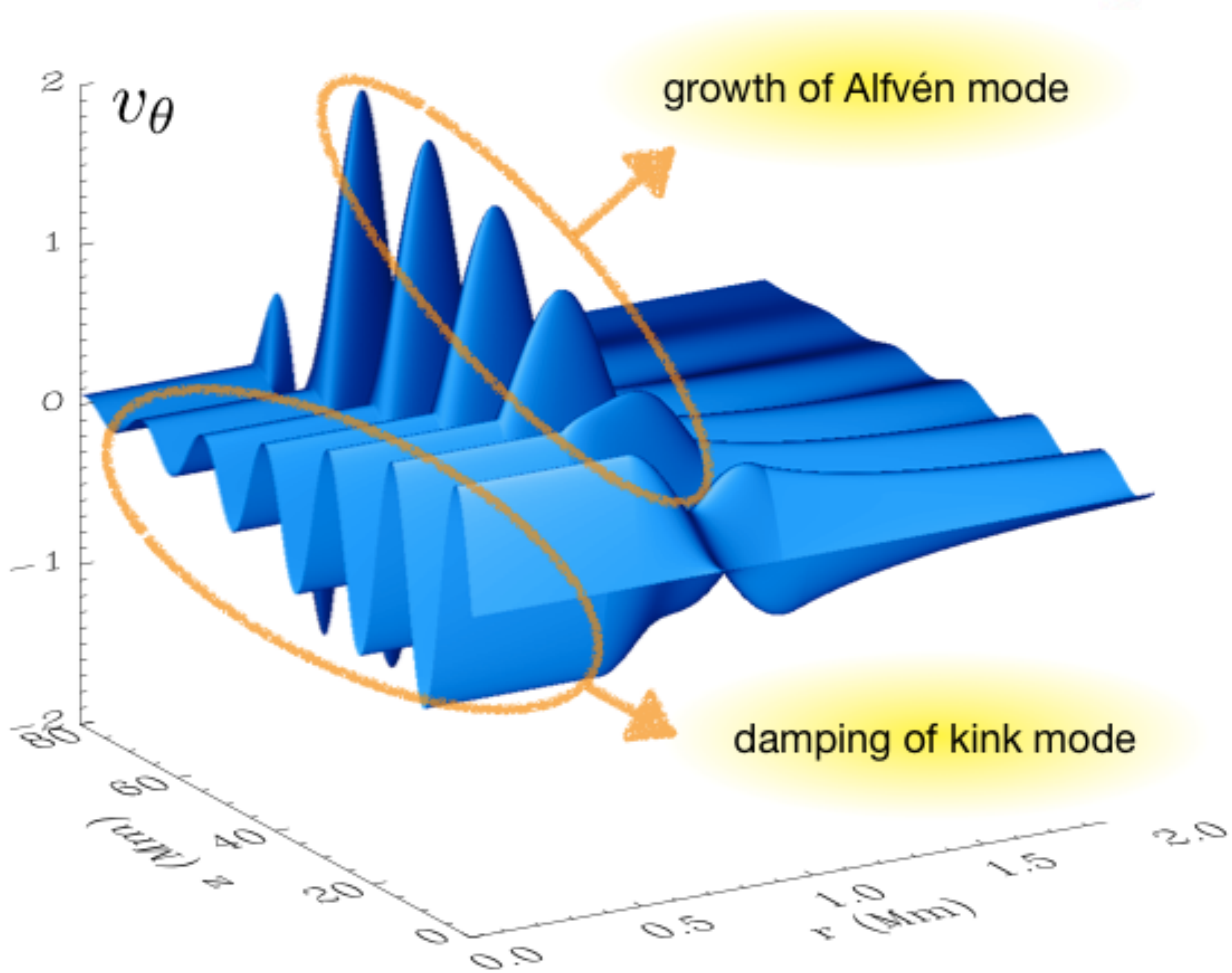

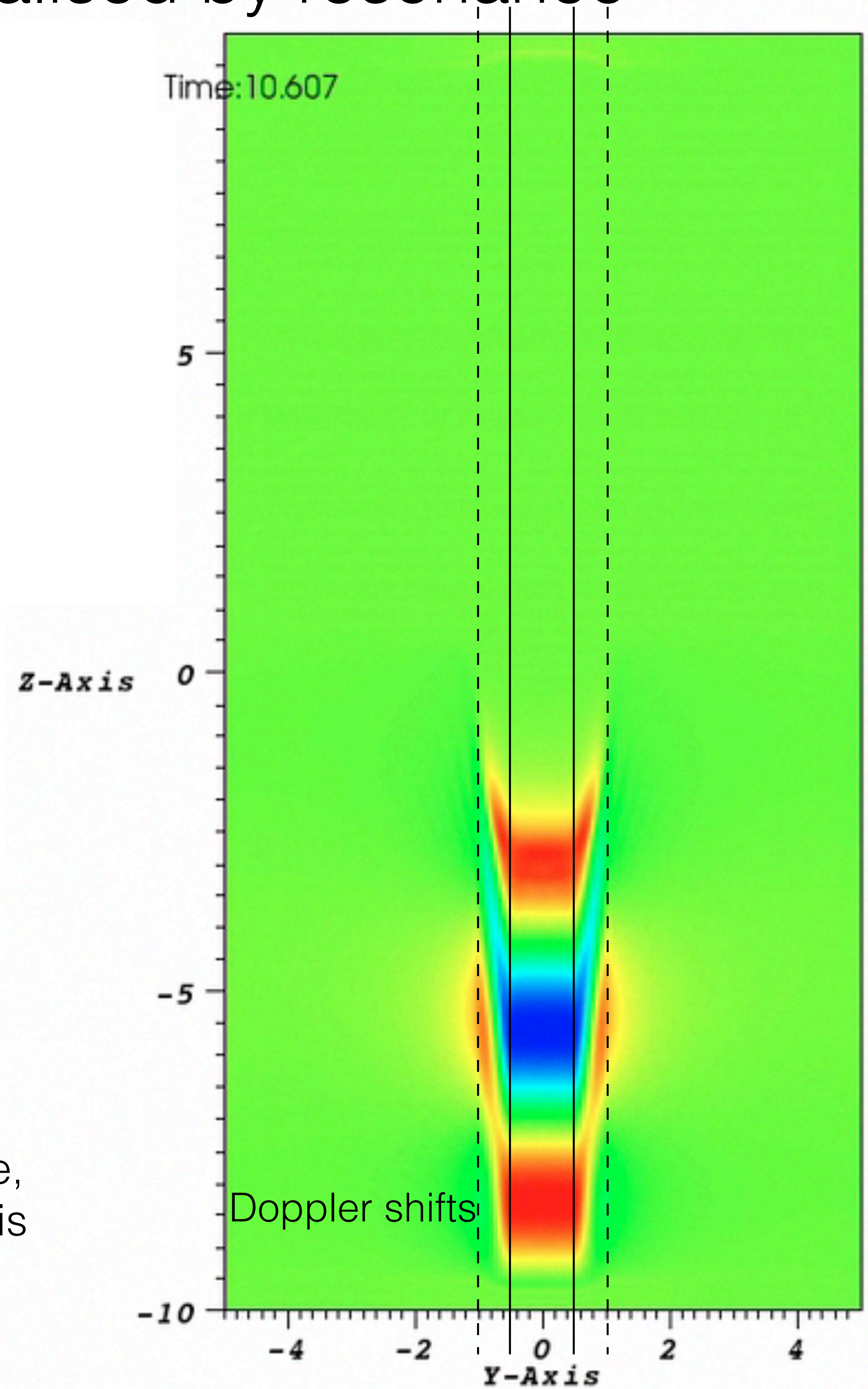

- Finite wave energy in system ("kick" given by the CME) so kink wave damps as Alfvén wave grows

- Alfvén wave is difficult to observe (incompressible, weak Doppler signal) so only damped kink wave is seen

Damping of kink waves by resonant absorption

- The **inhomogeneous layer** provides a continuous range of Alfvén speeds, and resonance occurs where the Alfvén speed equals the kink speed

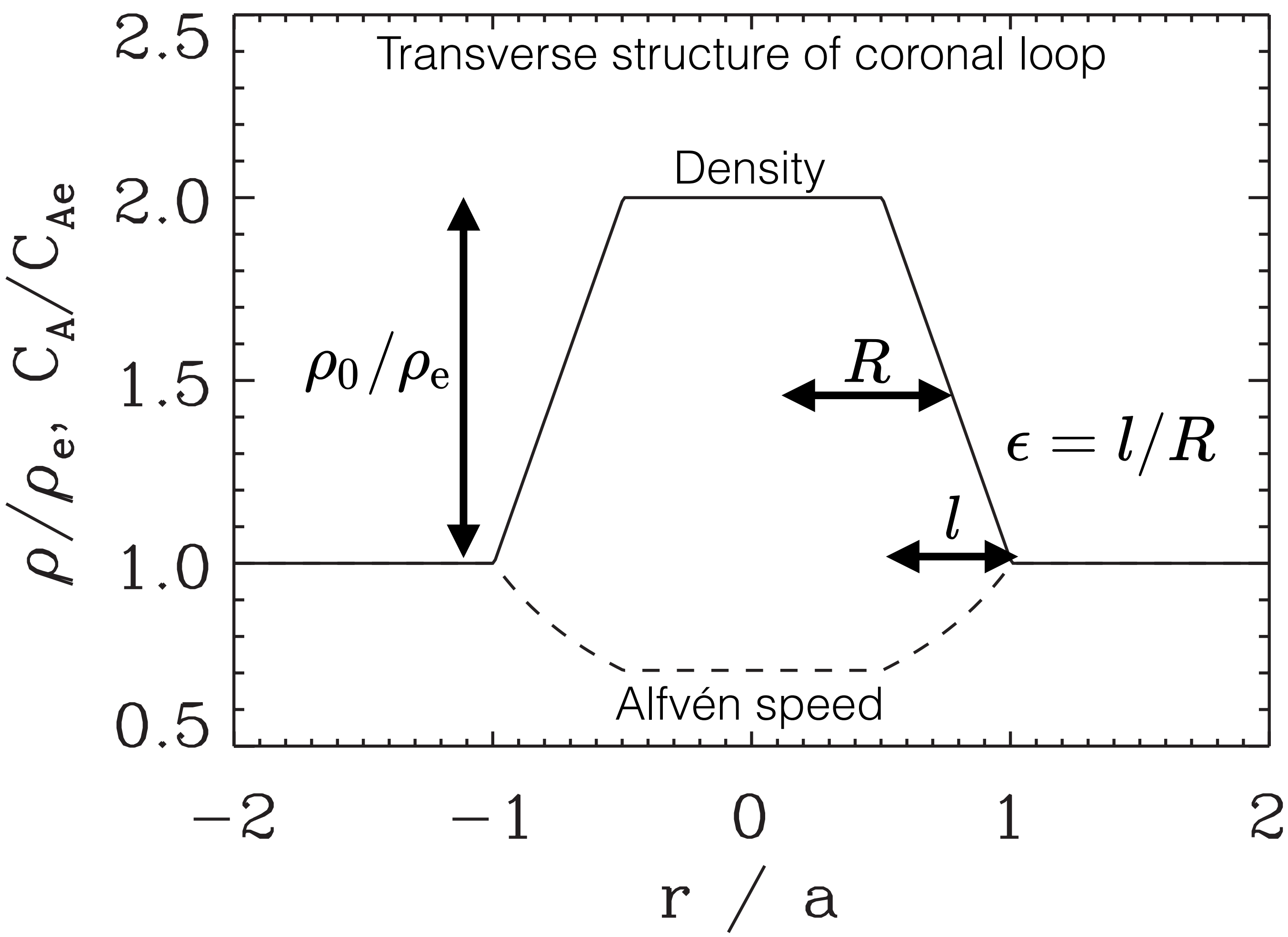

- Resonant absorption transfers energy from kink mode (collective motion) to Alfvén mode (localised, unresolved motion)

- Kink mode impulsively excited so transfer of wave energy to Alfvén mode causes damped kink oscillations

What is the kink mode damping envelope?

- Original application to coronal loops describes exponential damping envelope for kink oscillation:

$$A \propto \exp\left(-\frac{t}{\tau_\mathrm{d}}\right) \qquad \tau_\mathrm{d} \propto \frac{1}{\epsilon}\,\frac{\rho_0/\rho_\mathrm{e}+1}{\rho_0/\rho_\mathrm{e}-1}$$

Ruderman & Roberts (2002)
Goossens et al. (2002)

- Seismological inversion problem is ill-posed since τ_d (one observable) depends on density contrast ratio and ε (two unknowns)

Arregui et al. (2007)
Goossens et al. (2008)

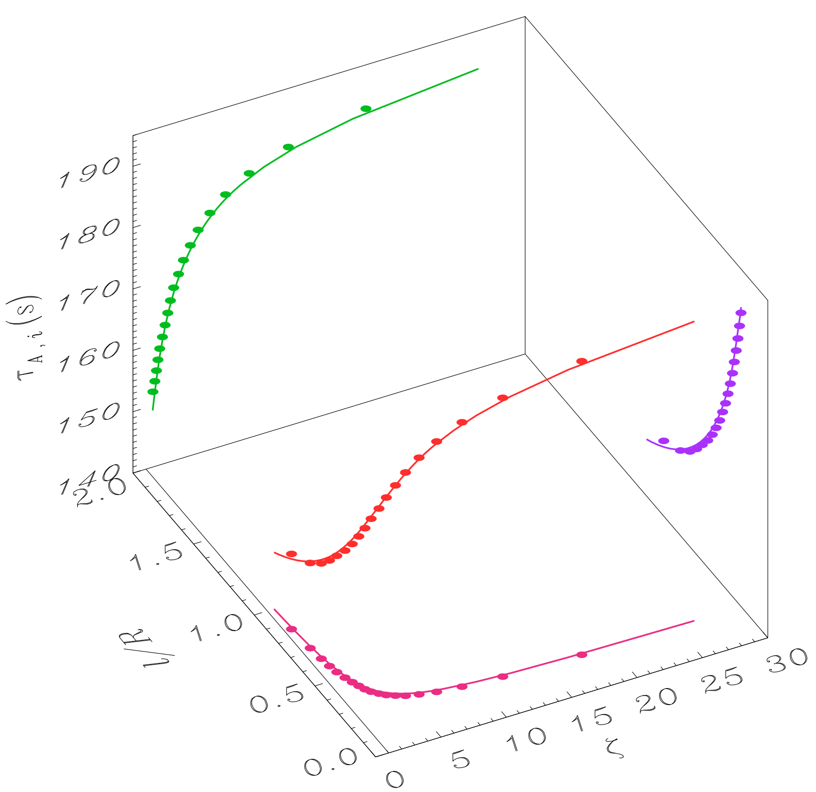

We consider this result in relation to the observational data reported by Nakariakov et al. (1999). These authors reported a coronal loop oscillation with frequency $\omega_k \approx 0.024\ \mathrm{s}^{-1}$ ($\tau = 256$ s) and decrement $\gamma \approx 0.0011\ \mathrm{s}^{-1}$ ($\tau_{\mathrm{decay}} = 870$ s). Taking $\rho_i = 10\rho_e$, we obtain from equation (72) that $\ell/a \approx 0.23$.

Ruderman & Roberts (2002)

- Inversion problem has infinite solutions, though bounding values can be estimated (e.g. Arregui & Asensio Ramos 2014)

What is the kink mode damping envelope?

- Numerical simulations of kink oscillations in low density contrast loops discovered Gaussian damping regime:

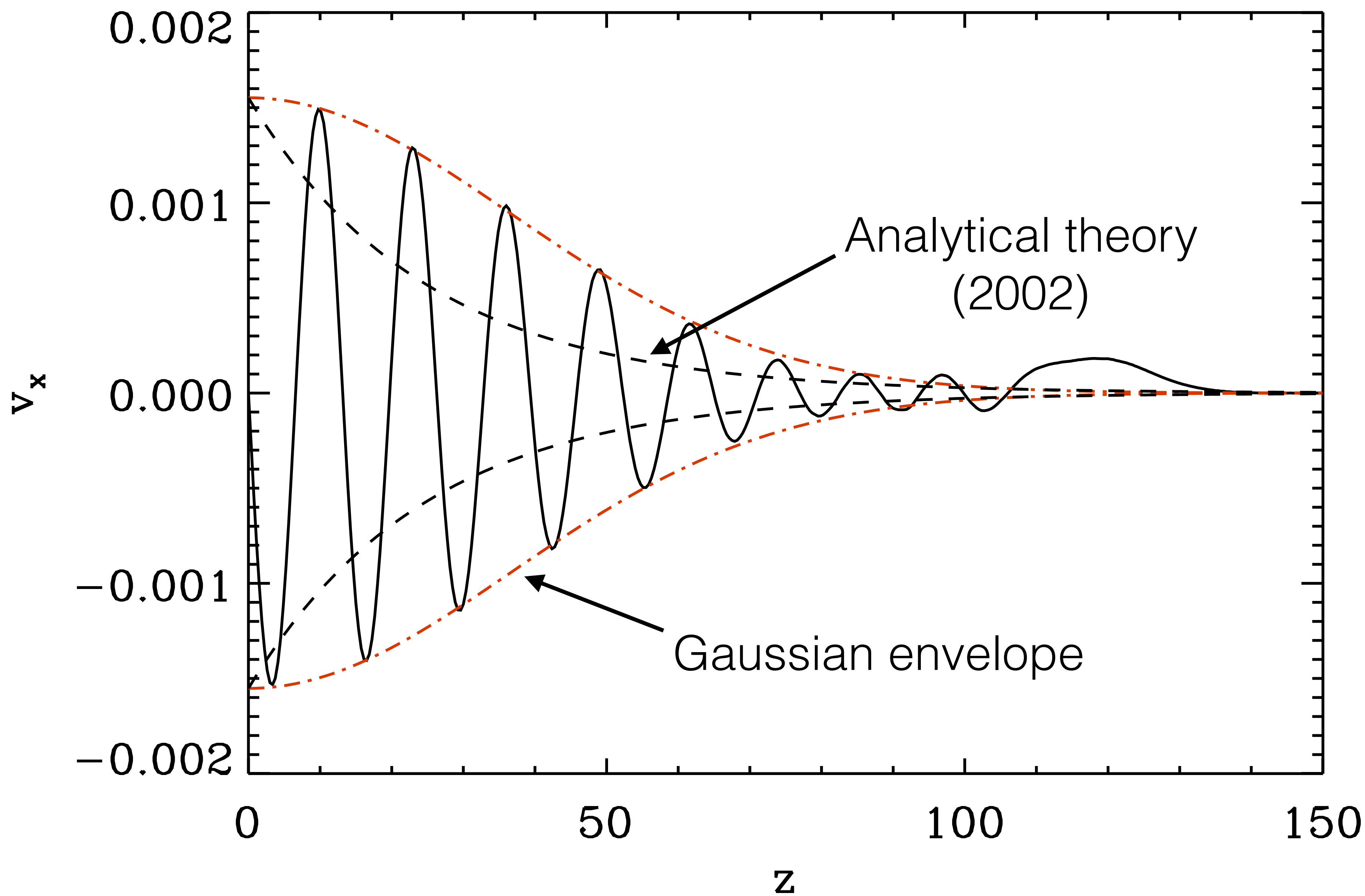

Pascoe et al. (2012, A&A, 539, A37)

New theoretical damping envelope

- New analytical solution (Hood et al. 2013) gives accurate envelope for all times:

$$\frac{d\tilde{\eta}}{dZ} = \frac{\epsilon}{2}\left\{\frac{a(1-\cos Z)}{Z} - \int_0^Z \tilde{\eta}(u)\frac{\sin(Z-u)}{Z-u}du\right\}$$

- Integro-differential equation allows precise testing of numerical simulations
- Gaussian profile describes initial state of the system
- Exponential damping profile describes asymptotic state of the system
- Inconvenient for seismological inversions for observations (solved numerically → slow)

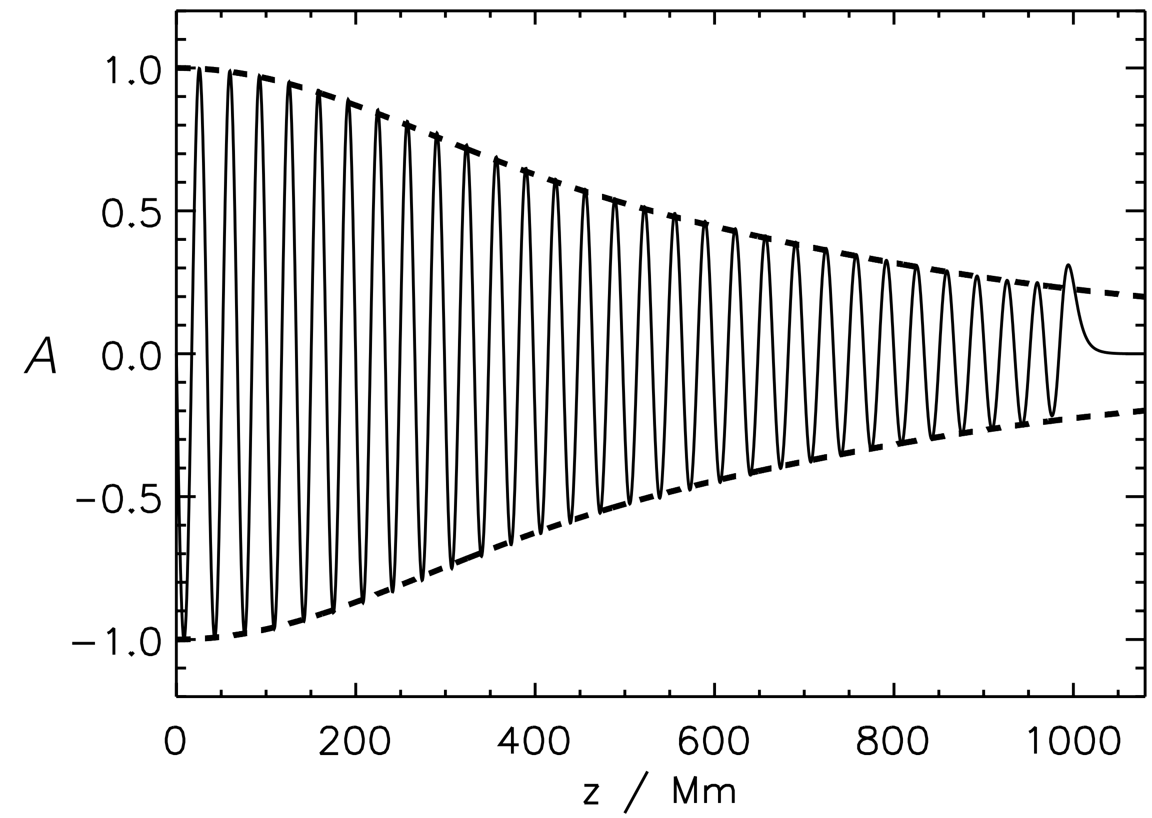

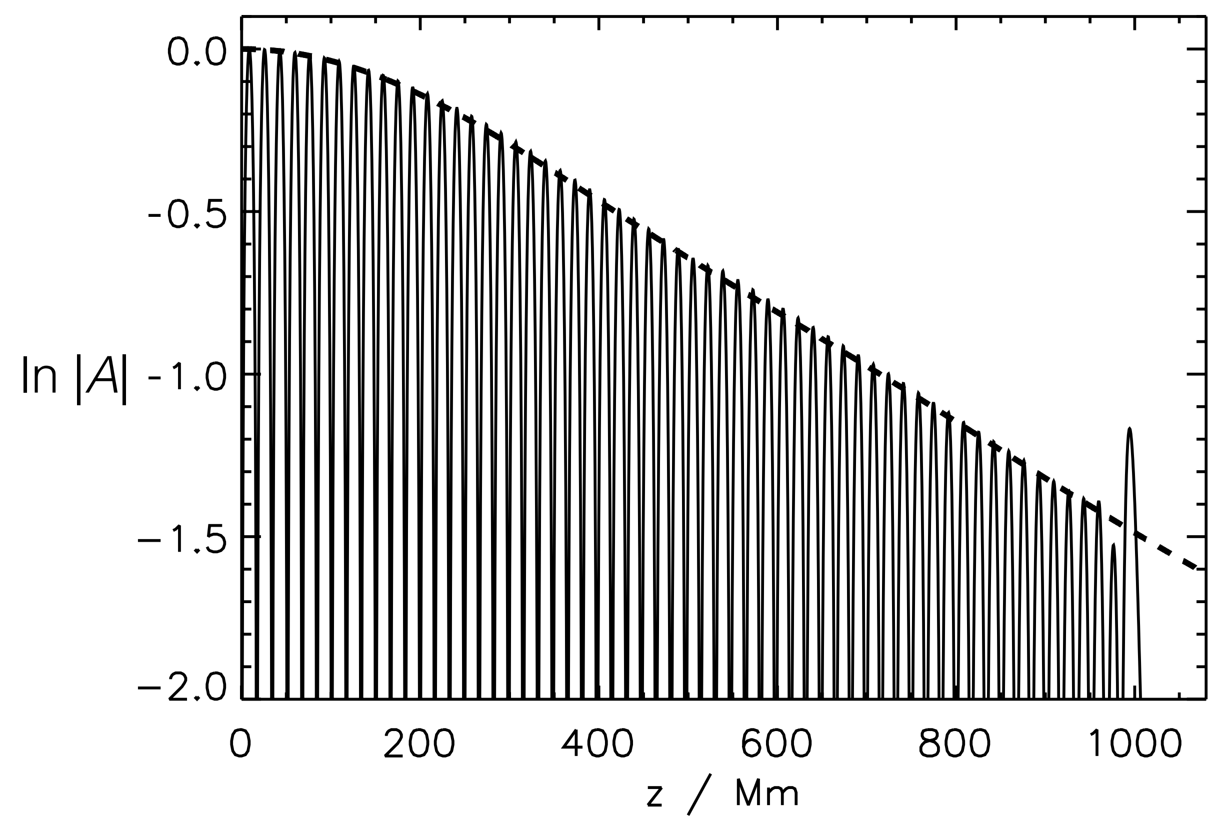

Hood et al. (2013, A&A, 551, A39)

Approximate damping envelope for seismology

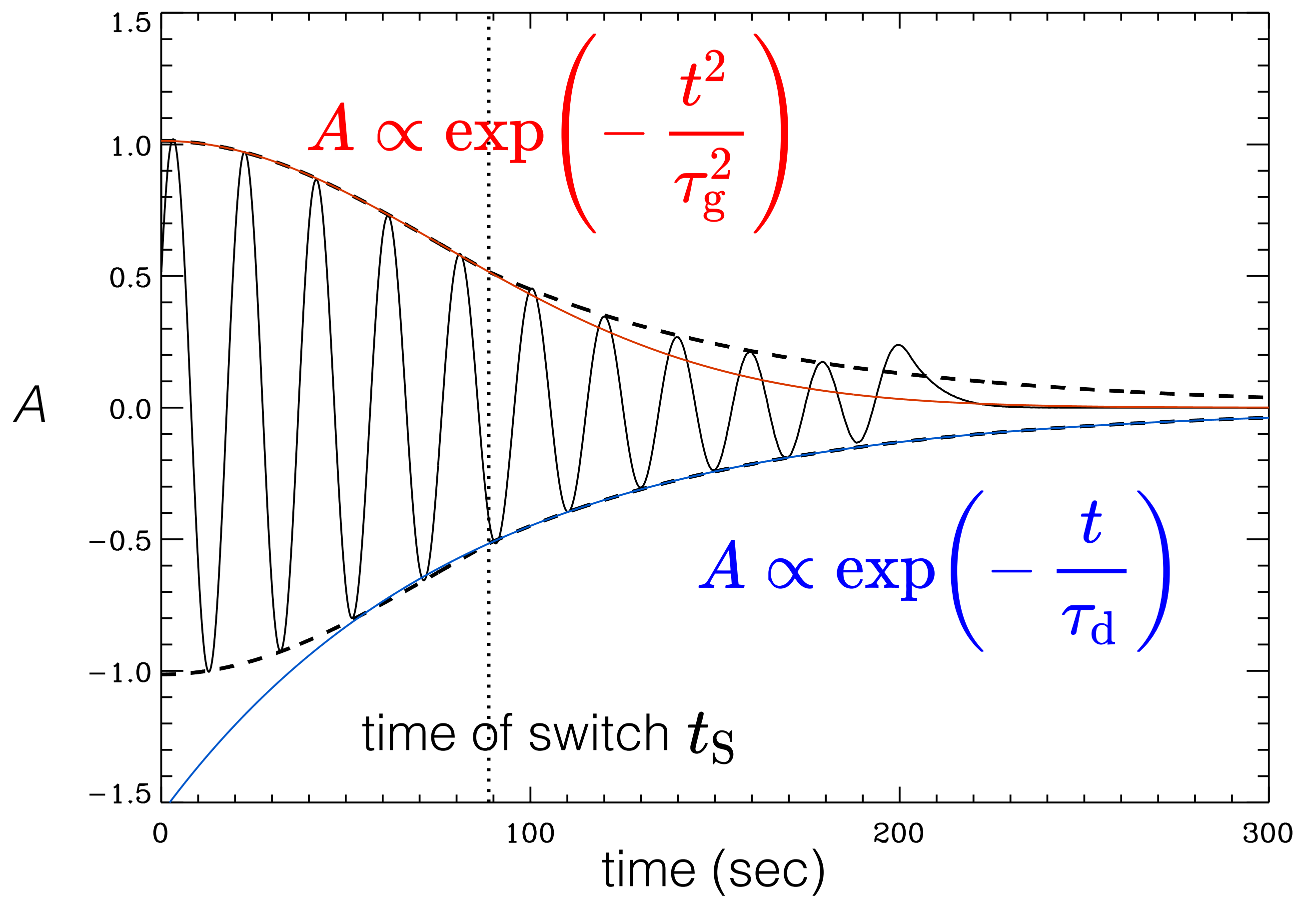

Numerical simulation of a kink mode showing **both** Gaussian and exponential damping regimes

$$t_s = \tau_g^2/\tau_d$$

- Time of switch depends on density contrast ratio:
  - small density contrast (~2) → slow switch → mostly Gaussian envelope
  - large density contrast (~10) → quick switch → mostly exponential envelope
- If we detect both envelopes we have **two damping times** (well-posed inversion problem) → unique solution for density contrast ratio and transition layer width

Hood et al. (2013)
Pascoe et al. (2013)

Gaussian damping regime for standing kink modes

- Same physical mechanism applies to standing modes

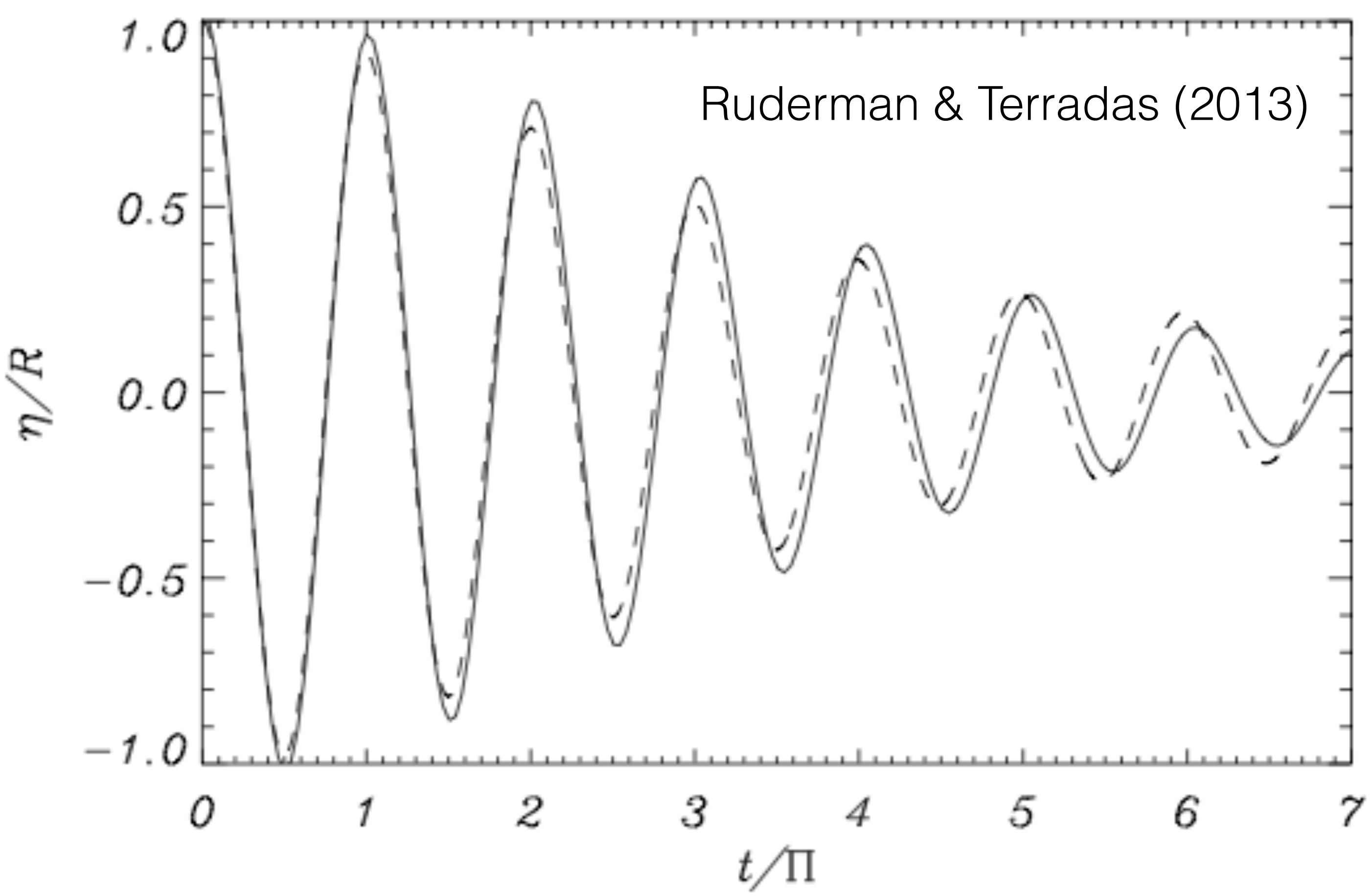

$$\frac{\tau_g}{P} = \frac{L_g}{\lambda} = \frac{2}{\pi\kappa\epsilon^{1/2}}$$

Pascoe et al. (2013)

- For standing kink modes, a large density contrast is usually assumed (typically 10, e.g., Nakariakov et al. 1999; Ruderman & Roberts 2002; Goossens et al. 2002)

- This density contrast is consistent with an exponential damping profile (Gaussian profile for ~ 1.2 oscillations only)

Evidence of Gaussian damping regime from TRACE

- De Moortel et al. (2002) and Ireland and De Moortel (2002) analyse standing kink oscillations

- Shape of damping envelope taken to be a fitted parameter

$$\propto \exp\left(-kt^N\right)$$

- 14 July 1998: $N \approx 2.0 \pm 1.2$

- 25 October 1999: $N \approx 0.43 \pm 1.17$

- 21 March 2001: $N \approx 2.0 \pm 1.3$

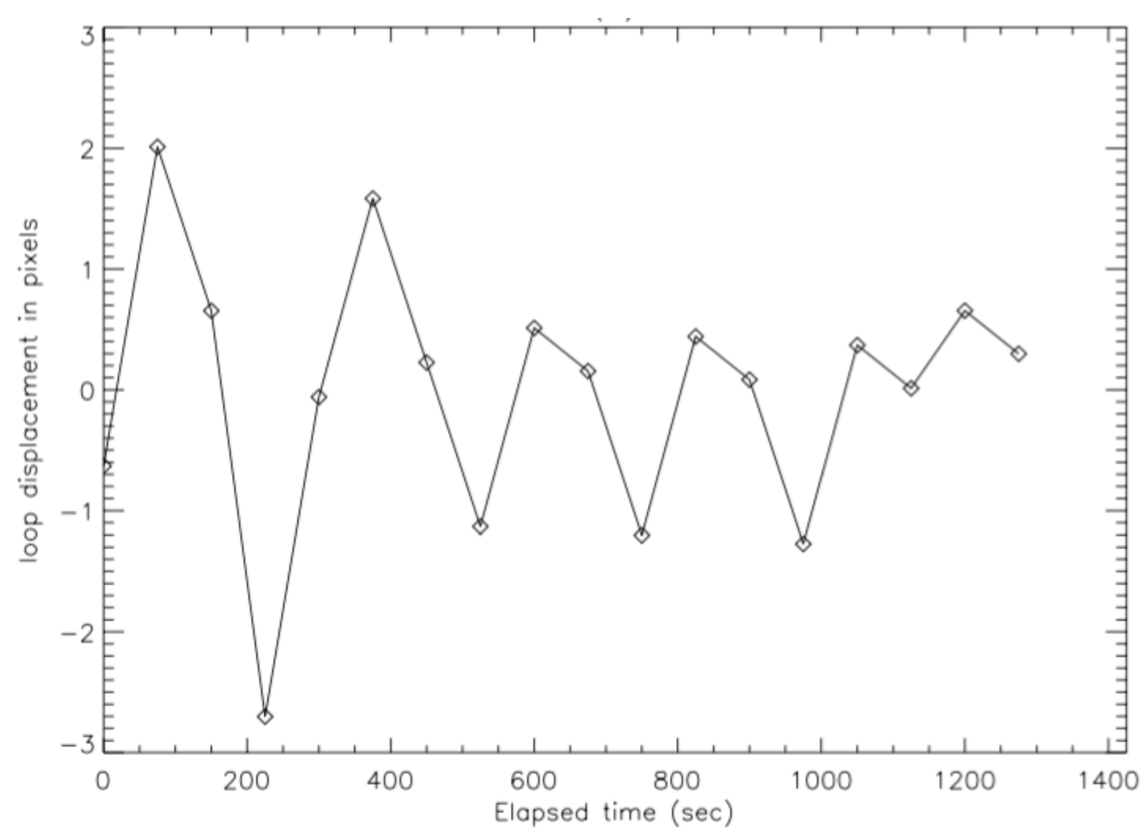

- Large errors due to low temporal resolution and noise for TRACE

Strongly damped kink oscillations

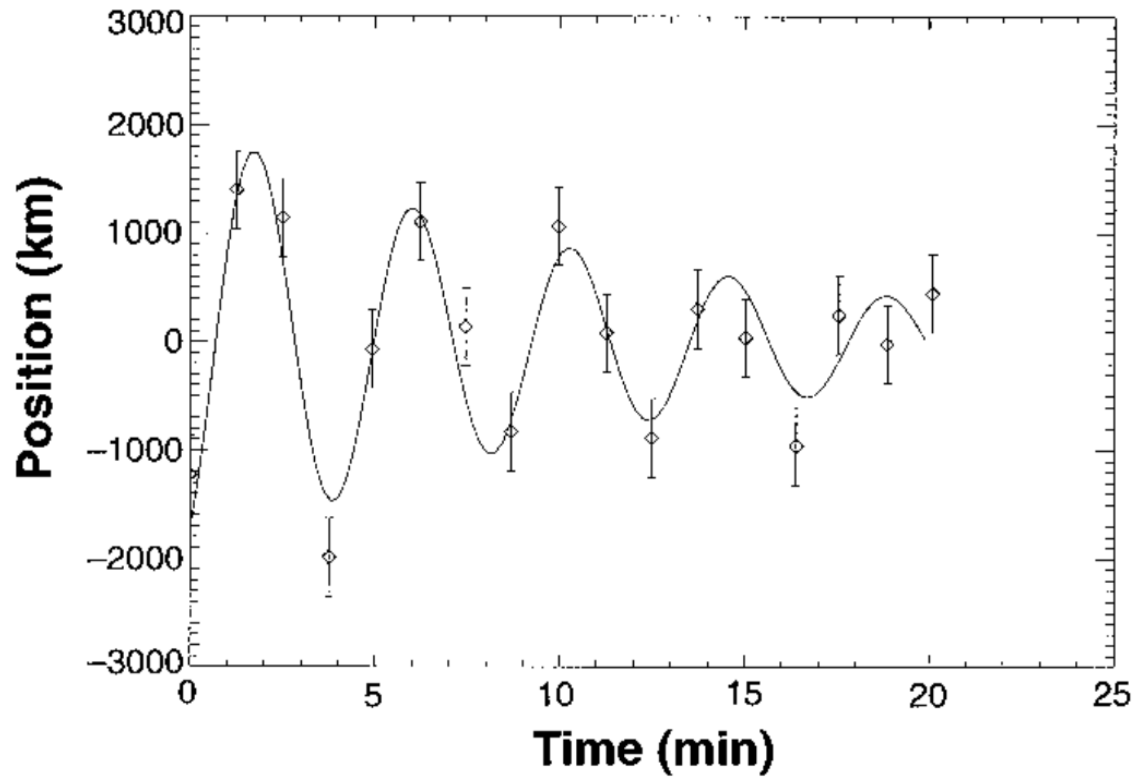

TRACE

0.5 arcsec/pixel

~75 second cadence

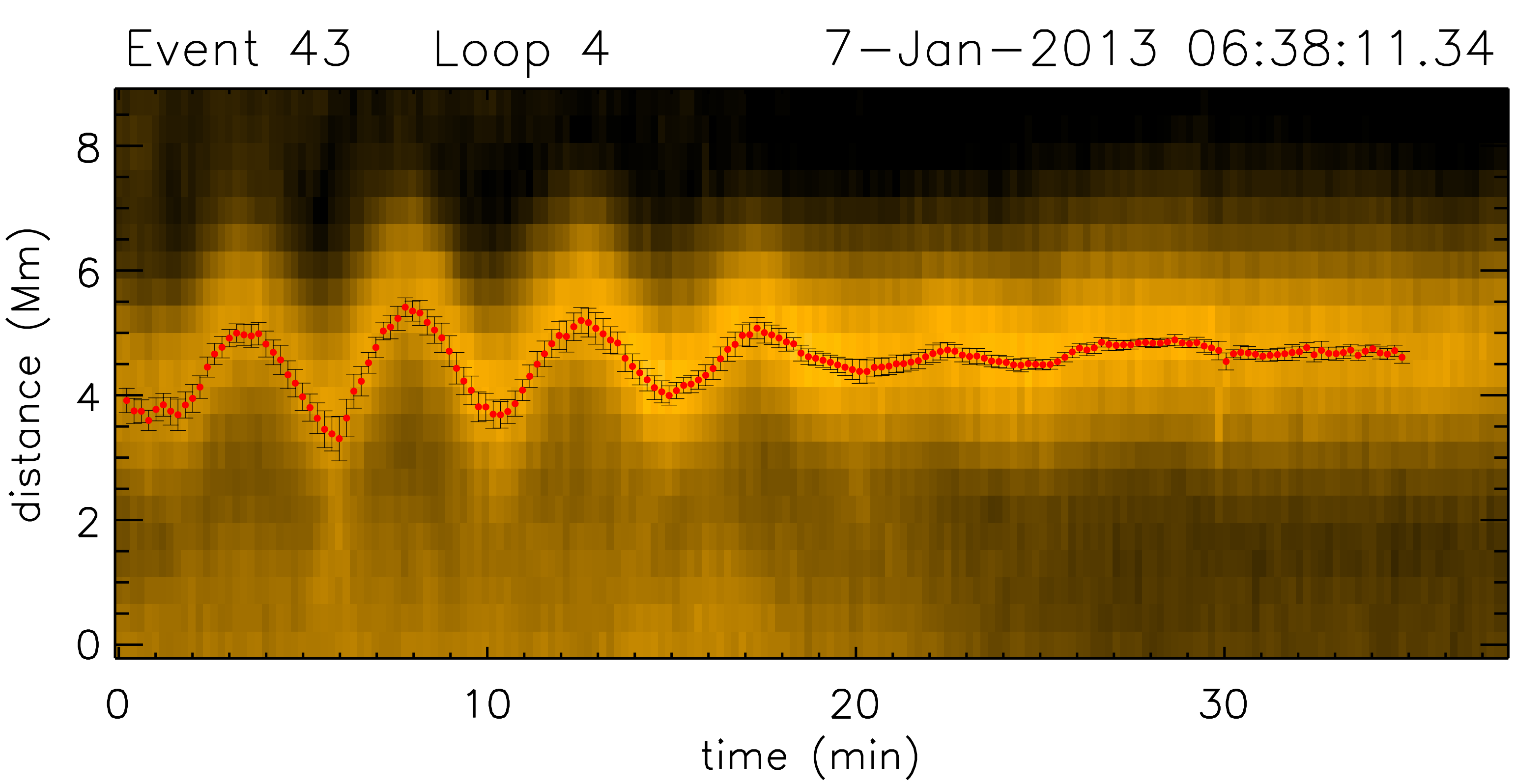

SDO/AIA

0.6 arcsec/pixel (full disk)

12 second cadence

Evidence of Gaussian damping regime from SDO

- Catalogue of 121 kink oscillations (Zimovets & Nakariakov 2015; Goddard et al. 2015) observed by SDO
  - 48 exponential profiles measured, 21 possible Gaussian profile

A&A 585, A137 (2016)

Appendix A: Table

Table A.1. 120 coronal loop kink oscillations detected with SDO/AIA and their measured parameters.

Event ID	Loop ID	Slit position [x1, y1, x2, y2] (arcsec)	Date	Time UT	Period (min)	Length (Mm)	Disp amp (Mm)	Osc amp (Mm)	N Cyc	Damping time (min)	Damping profile
1	1	−940, −321, −964, −308	2010-Aug-02	04:22:49	3.42 ± 0.06	232	5.1	1.7	3	5.34 ± 1.12	E
1	2	−962, −313, −997, −322	2010-Aug-02	04:22:13	4.11 ± 0.05	78	7.0	1.2	3	10.76 ± 2.79	E
2	1	672, −259,711, −223	2010-Oct-12	19:13:07	6.64 ± 0.06	156	2.0	4.8	3.5		
3	1	−977, −383, −988, −368	2010-Nov-03	12:13:48	2.46 ± 0.03	213	1.4	4.7	8	8.8 ± 1.8	E, NE
3	2	−970, −416, −1001, −393	2010-Nov-03	12:14:35	3.62 ± 0.08	262	4.4	9.7	3	4.12 ± 0.47	E, NE
3	3	−978, −466, −1027, −411	2010-Nov-03	12:14:23	4.04 ± 0.1	311	4.1	8.9	2		
4	1	912, 405, 889, 433	2011-Feb-09	01:30:02	2.29 ± 0.03	183	2.9	4.4	4.5	7.18 ± 1.5	E, NE
4	2	969,231,974,278	2011-Feb-09	01:31:54	3.47 ± 0.03	181	1.4	1.2	3	7.44 ± 1	E
5	1	1089, 375, 1050, 423	2011-Feb-10	04:43:38	7.03 ± 0.06	438	4.5	3.0	3		NE
6	1	1089, 349, 1057, 398	2011-Feb-10	06:44:22	8.05 ± 0.26	430	3.8	0.5	2		
7	1	983, 330, 970, 342	2011-Feb-10	06:57:46	1.69 ± 0.02	162	2.9	3.2	6	7.23 ± 1.3	E, NE
8	1	1007, 280, 1021, 305	2011-Feb-10	12:35:01	3.74 ± 0.07	207	1.2	1.6	3	10 ± 1	E, NE
9	1	983, 348, 947, 414	2011-Feb-10	13:43:37	5.14 ± 0.17	264	3.0	4.3	3	5.09 ± 0.98	E
9	2	942,431,934,461	2011-Feb-10	13:46:31	8.95 ± 0.14	326	3.6	3.2	2.5	11.83 ± 4.76	E
10	1	1106, 168, 1133, 214	2011-Feb-11	08:07:07	11.46 ± 0.17	397	4.7	8.9	2.5	8.02 ± 1.09	E, NE
10	2	1039, 313, 1041, 334	2011-Feb-11	08:08:17	8.48 ± 0.16	279	5.9	6.0	2		
11	1	−41, −162, −43, −146	2011-Feb-13	17:34:28	3.96 ± 0.07	78	3.5	4.4	3		
11	2	−49, −132, −51, −108	2011-Feb-13	17:34:50	3.85 ± 0.11	95	3.7	2.1	3		
11	3	−64, −334, −69, −316	2011-Feb-13	17:37:13	2.6 ± 0.05	118	3.1	3.7	6	8.84 ± 1.5	E
11	4	−41, −334, −54, −322	2011-Feb-13	17:33:52	3.81 ± 0.04	125	2.9	5.4	5		
11	5	−24, −359, −44, −336	2011-Feb-13	17:33:42	5.09 ± 0.06	135	1.9	6.3	2		
11	6	−98, −430, −89, −394	2011-Feb-13	17:38:33	6.13 ± 0.21	160	11.2	11.1	2		
12	1	−282, −37, −309, −47	2011-Feb-13	20:19:17	5.56 ± 0.07	148	1.9	1.8	2		
15	1	202, 313, 175, 371	2011-May-27	10:47:58	7.64 ± 0.37	174	6.3	6.2	1.5		
16	1	1014, 235, 991, 257	2011-Aug-11	10:17:19	2.62 ± 0.04	242	3.3	3.1	3		
16	2	988, 229, 1026, 229	2011-Aug-11	10:10:22	2.35 ± 0.07	146	17.4	3.2	2	2.69 ± 0.64	E
16	3	1031, 205, 1067, 241	2011-Aug-11	10:10:54	5.23 ± 0.19	318	25.5	5.2	2.5		
17	1	231, 215, 216, 263	2011-Sep-06	22:20:15	2.07 ± 0.04	153	9.5	3.4	3.5	9.99 ± 4.59	E
18	1	−931,431, −960,472	2011-Sep-22	10:35:08	7.18 ± 0.32	289	15.8	10.0	2.5		
18	2	−911,457, −884,476	2011-Sep-22	10:26:59	9.52 ± 0.11	284	1.4	1.7	3.5	12.2 ± 3.47	E
18	3	−1093,290, −1060,320	2011-Sep-22	10:30:32	13.02 ± 0.17	393	4.9	9.5	4		NE
19	1	−954,158, −998,134	2011-Sep-23	23:51:45	9.73 ± 0.2	123	4.7	2.9	2		
19	2	−938, −31, −992, −12	2011-Sep-23	23:51:57	11.27 ± 0.12	348	7.5	10.0	2	16.55 ± 1.44	E
20	1	−676, −12, −682,62	2011-Nov-14	07:21:12	5.36 ± 0.23	253	2.6	3.7	3	16.19 ± 7.67	E, NE
20	2	−616, −171, −665, −161	2011-Nov-14	00:05:04	13.43 ± 0.67		4.3	4.0	2		
21	1	920, 693, 907, 725	2011-Nov-16	14:08:19	7.15 ± 2.01	499	1.8	3.8	2		
22	1	995, 340, 1004, 332	2011-Nov-16	14:56:05	2.7 ± 0.11	288	1.6	1.8	3		
23	1	827,662,813,699	2011-Nov-17	22:28:37	15.36 ± 0.4	365	6.4	4.3	3	19.19 ± 1.55	E
23	2	920, 744, 856, 729	2011-Nov-17	22:32:49	28.19 ± 0.51		12.1	4.9	2.5		
24	1	−881, −588, −910, −549	2011-Nov-18	07:34:59	17.86 ± 0.3	432	14.5	15.6	3	27.43 ± 4.26	E
24	2	−848, −608, −901, −572	2011-Nov-18	07:29:42	16.45 ± 0.28	427	21.8	23.6	3		
24	3	−814, −673, −894, −645	2011-Nov-18	07:36:02	20.46 ± 0.58	538	31.8	26.6	2	35.01 ± 6.44	E
25	1	316, −221,321, −195	2011-Dec-22	01:59:34	5.13 ± 0.11	156	2.0	3.0	3	8 ± 5	E, NE
25	2	272, −141,332, −92	2011-Dec-22	01:59:39	7.3 ± 0.16	264	1.8	2.5	2.5		
26	1	1098, 13, 1126, 51	2012-Jan-16	00:08:28	11.95 ± 0.13	473	2.5	9.2	4.5	18.71 ± 4.5	E, NE
26	2	1028, −68,1025, −33	2012-Jan-16	00:11:27	12.51 ± 0.19	185	2.3	6.6	4		NE
27	1	1042, 93, 1072, 146	2012-Apr-09	01:19:52	15.28 ± 0.4	244	4.3	3.2	3		
29	1	−633,339, −628,380	2012-May-08	13:05:46	3.71 ± 0.05	154	7.4	5.3	6	7.83 ± 0.62	E
31	1	964,289,945,325	2012-May-26	20:36:47	7.67 ± 0.04	162	19.6	9.4	6	24.22 ± 2.02	E
31	2	944, 259, 944, 284	2012-May-26	20:36:27	9.59 ± 0.09	138	13.0	9.1	5	17.57 ± 2.35	E, NE
31	3	1116,286,1112,330	2012-May-26	20:39:53	11.56 ± 0.12	532	4.5	2.7	2.5		
32	1	−973, −366, −988, −342	2012-May-30	08:58:57	4.28 ± 0.02	234	2.2	8.8	8	15.55 ± 1.22	E
32	2	−972, −388, −989, −370	2012-May-30	08:56:52	3.38 ± 0.02	233	4.0	5.3	5	19.11 ± 4.85	E
33	1	807, −608,840, −591	2012-Jul-06	23:06:45	4.69 ± 0.08	314	7.0	8.6	2.5		
33	2	867, −101,874, −45	2012-Jul-06	23:05:07	6.52 ± 0.1	407	8.5	7.7	3		E
34	1	−1053, −142, −1076, −129	2012-Aug-07	00:59:34	9.95 ± 0.27	333	15.4	7.4	2.5	16.7 ± 1.03	E

Notes. The event ID corresponds to the events catalogued in Zimovets & Nakariakov (2015), and the loop ID distinguishes the different loops in each event (which does not correspond to those in the cited paper). The position of the slit used to produce each time-distance map is given in arcsec, along with the date and oscillation start time in UT. The period and error obtained from fitting the loop oscillation are given, as well as the estimated loop length. The column "Disp Amp" lists the estimated initial loop displacement, and "Osc Amp" is the estimated initial amplitude of the oscillation. The number of cycles that were observed is listed in "N Cyc". Finally, the exponential damping time and error from fitting the damping profile and the form of the damping profile (exponential (E), non-exponential (NE), or a combination of both), are listed in the final two columns.

A137, page 8 of 9

C. R. Goddard et al.: Kink oscillations – a statistical study

Table A.1. continued.

Event ID	Loop ID	Slit position [x1, y1, x2, y2] (arcsec)	Date	Time UT	Period (min)	Length (Mm)	Disp amp (Mm)	Osc amp (Mm)	N Cyc	Damping time (min)	Damping profile
35	1	−1024, −148,-1037, −110	2012-Aug-07	01:34:47	8.78 ± 0.13	327	1.9	3.0	3		
35	2	−1033, −185, −1070, −185	2012-Aug-07	01:33:52	5.77 ± 0.1	312	1.4	2.8	2.5		
36	1	−1018, −152, −1039, −112	2012-Aug-07	03:03:46	6.68 ± 0.1	282	1.3	3.8	4		
37	1	−1110,66, −1103,87	2012-Oct-15	21:52:17	8.27 ± 0.22	358	2.3	3.8	2.5		
38	1	−1046, −180, −1046, −159	2012-Oct-19	19:01:00	3.04 ± 0.03	224	2.7	1.6	4		
38	2	−1061, −201, −1065, −174	2012-Oct-19	19:01:44	5.2 ± 0.08	270	3.0	2.1	3	15.23 ± 5.5	E, NE
38	3	−1121, −189, −1142, −175	2012-Oct-19	19:03:00	13.08 ± 0.21	424	5.2	4.9	2		
38	4	−1139, −194, −1162, −185	2012-Oct-19	19:01:08	10.74 ± 0.18	478	5.0	5.8	2		
39	1	−1093, −124, −1140, −107	2012-Oct-19	21:04:19	10.79 ± 0.1	402	6.5	4.1	4.5		NE
39	2	−1088, −185, −1095, −157	2012-Oct-19	21:01:34	10.68 ± 0.12	334	2.0	1.9	5		NE
39	3	−1095, −204, −1120, −172	2012-Oct-19	21:03:44	12.57 ± 0.36	376	2.3	3.5	3.5		
39	4	−1127, −168, −1161, −179	2012-Oct-19	21:00:40	14.3 ± 0.17	454	3.7	3.5	4		NE
40	1	−1025, −63, −1037, −47	2012-Oct-20	18:07:36	5.68 ± 0.06	171	1.4	1.7	4		
40	2	−1077, −121, −1065, −96	2012-Oct-20	18:09:33	5.61 ± 0.03	347	9.6	4.4	7	24.83 ± 3.41	E, NE
40	3	−1073, −136, −1058, −120	2012-Oct-20	18:11:36	5.92 ± 0.7	325	2.6	3.0	4		
40	4	−1045, −114, −1020, −110	2012-Oct-20	18:10:08	5.53 ± 0.04	258	3.6	2.5	6	7.32 ± 1.08	E, NE
40	5	−1056, −122, −1043, −115	2012-Oct-20	18:12:55	5.42 ± 0.02	297	3.9	4.7	6		
40	6	−1095, −123, −1079, −101	2012-Oct-20	18:09:59	6.93 ± 0.04	425	6.2	3.5	11		NE
40	7	−1107, −153, −1094, −121	2012-Oct-20	18:11:11	5.72 ± 0.06	353	3.1	3.4	12	14.17 ± 2.73	E, NE
40	8	−1036, −217, −1066, −194	2012-Oct-20	18:08:39	4.33 ± 0.08	238	10.3	12.1	4.5	9.01 ± 2.16	E, NE
40	9	−1109, −438, −1117, −399	2012-Oct-20	18:11:45	6.18 ± 0.05	473	12.5	13.7	3.5	13.15 ± 2.66	E
40	10	−962, −430, −982, −453	2012-Oct-20	18:12:21	6.27 ± 0.03	238	2.2	2.1	10		NE
40	11	−978, −404, −999, −418	2012-Oct-20	18:11:29	4.76 ± 0.04	220	1.6	1.3	4		
43	1	933,615,894,615	2013-Jan-07	06:37:38	7.14 ± 0.07	363	8.0	16.3	5	7.53 ± 1.45	E
43	2	874,598,890,613	2013-Jan-07	06:37:50	3.6 ± 0.03	241	9.7	3.1	5	9.44 ± 0.92	E
43	3	828,659,816,708	2013-Jan-07	06:39:19	8.35 ± 0.08	368	2.1	12.7	3.5	15.04 ± 1.81	E
43	4	829,606,826,620	2013-Jan-07	06:37:01	5.16 ± 0.03	222	3.9	3.5	4		
43	5	801,608,812,631	2013-Jan-07	06:37:11	4.5 ± 0.02	260	1.3	2.2	5.5	14 ± 2	E, NE
44	1	829,644,820,687	2013-Jan-07	08:48:37	7.23 ± 0.06	295	2.8	12.3	5	15.75 ± 3.09	E
44	2	979,637,940,676	2013-Jan-07	08:48:17	9.78 ± 0.19	512	15.8	13.4	3	14.62 ± 4.96	E, NE
44	3	886,644,936,622	2013-Jan-07	08:47:19	6.95 ± 0.14	352	17.2	4.8	4	9 ± 3	
44	4	869,575,879,587	2013-Jan-07	08:48:53	2.41 ± 0.05	202	2.9	2.8	4		
45	1	−396,367, −409,379	2013-Feb-17	15:45:42	2.48 ± 0.04	92	0.7	3.1	3.5	7.82 ± 1.66	E
46	1	−1024, −281, −1038, −268	2013-May-24	18:55:12	12.07 ± 0.23	430	1.5	4.4	2.5		
46	2	−1102, −389, −1080, −363	2013-May-24	18:53:58	10.99 ± 0.11	498	2.4	3.7	5		NE
46	3	−1032, −332, −1054, −327	2013-May-24	18:54:34	9.9 ± 0.1	384	2.5	3.8	6		NE
47	1	207, −251,223, −243	2013-May-27	01:53:28	5.27 ± 0.14	225	0.6	1.6	3		
47	2	237, −197,270, −188	2013-May-27	02:02:59	5.02 ± 0.12	222	2.9	1.6	3		
48	1	−1076,77, −1044,111	2013-Jul-18	17:59:56	15.28 ± 0.16	540	12.3	22.0	3.5	21.98 ± 15.6	E, NE
48	2	−1134,36, −1069,99	2013-Jul-18	17:59:01	15.76 ± 0.12	588	25.4	27.4	5	26.64 ± 2.17	E, NE
48	3	−1153,41, −1102,112	2013-Jul-18	17:58:34	16.08 ± 0.21	597	19.9	23.7	4	15.76 ± 3.09	E
48	4	−1084, −59, −1069, −33	2013-Jul-18	17:56:10	9.23 ± 0.23	426	7.7	7.6	4		
48	5	−1139, −15, −1102,42	2013-Jul-18	17:57:31	15.83 ± 0.21	471	17.9	13.0	3.5		
49	1	−1041,93, −1117,118	2013-Oct-11	07:12:01	15.12 ± 0.47	484	13.6	22.9	2		
49	2	−1030, −126, −1058, −106	2013-Oct-11	07:15:17	7.73 ± 0.14	197	3.6	6.4	3		
49	4	−1044,409, −1082,429	2013-Oct-11	07:13:30	10.45 ± 0.17	386	17.9	8.0	3	15.38 ± 2.58	E
49	5	−1020, −76, −1071, −51	2013-Oct-11	07:15:51	8.03 ± 0.18	191	10.4	13.0	3	9.37 ± 1.22	E
52	1	−710,65, −721,113	2014-Jan-04	15:32:47	5.93 ± 0.12	183	3.0	12.5	3		
53	1	1101, −296,1136, −291	2014-Jan-06	07:42:35	9.48 ± 0.22	420	1.5	8.4	1.5		
54	1	1115,220,1143,254	2014-Feb-10	21:00:57	8.33 ± 0.07	408	1.3	3.2	3		
54	2	1118,55,1134,82	2014-Feb-10	21:01:06	7.46 ± 0.1	400	4.2	8.0	3		
54	3	1062,110,1078,106	2014-Feb-10	21:02:02	2.32 ± 0.05	238	1.0	0.9	3		
54	4	1108,29,1138,43	2014-Feb-10	20:58:27	3.77 ± 0.13	355	7.5	3.0	2		
54	5	1076, −6,1091,1	2014-Feb-10	20:59:10	4.8 ± 0.1	257	3.6	2.9	4.5	19.72 ± 3.23	E, NE
55	1	1123,231,1143,244	2014-Feb-10	22:48:05	8.63 ± 0.24	405	5.9	3.7	2.5		
55	2	1167,190,1203,192	2014-Feb-10	22:44:59	6.54 ± 0.17	477	1.9	2.8	3		
56	1	1124, −8,1186,1	2014-Feb-11	13:28:08	9.07 ± 0.14	403	9.3	7.8	4	20.71 ± 4.71	E, NE
56	2	1068, −39,1130, −6	2014-Feb-11	13:28:13	11.88 ± 0.13	314	17.8	27.6	5	19.62 ± 2.96	E
56	3	1027,82,1043,54	2014-Feb-11	13:26:19	3.22 ± 0.16	205	16.5	9.2	2.5		
56	4	1062,397,1122,348	2014-Feb-11	13:27:33	14.38 ± 0.34	501	16.2	23.2	2		
56	5	1026,332,1004,354	2014-Feb-11	13:28:38	13.5 ± 0.16	431	6.9	10.7	4.5	24.17 ± 5.13	E
56	6	998,318,979,345	2014-Feb-11	13:28:49	7.59 ± 0.2	392	3.6	3.8	2.5		
56	7	1068,427,1023,456	2014-Feb-11	13:31:32	14.16 ± 0.55	457	4.9	15.0	3	13.64 ± 3.93	E, NE
56	8	1015,384,990,419	2014-Feb-11	13:30:19	10.64 ± 0.15	379	3.5	9.0	4		

A137, page 9 of 9

- Pascoe et al. (2016, A&A, 585, L6) looked at 6 loops in detail
  - 3 Gaussian, 2 exponential, 1 inconclusive

Gaussian examples

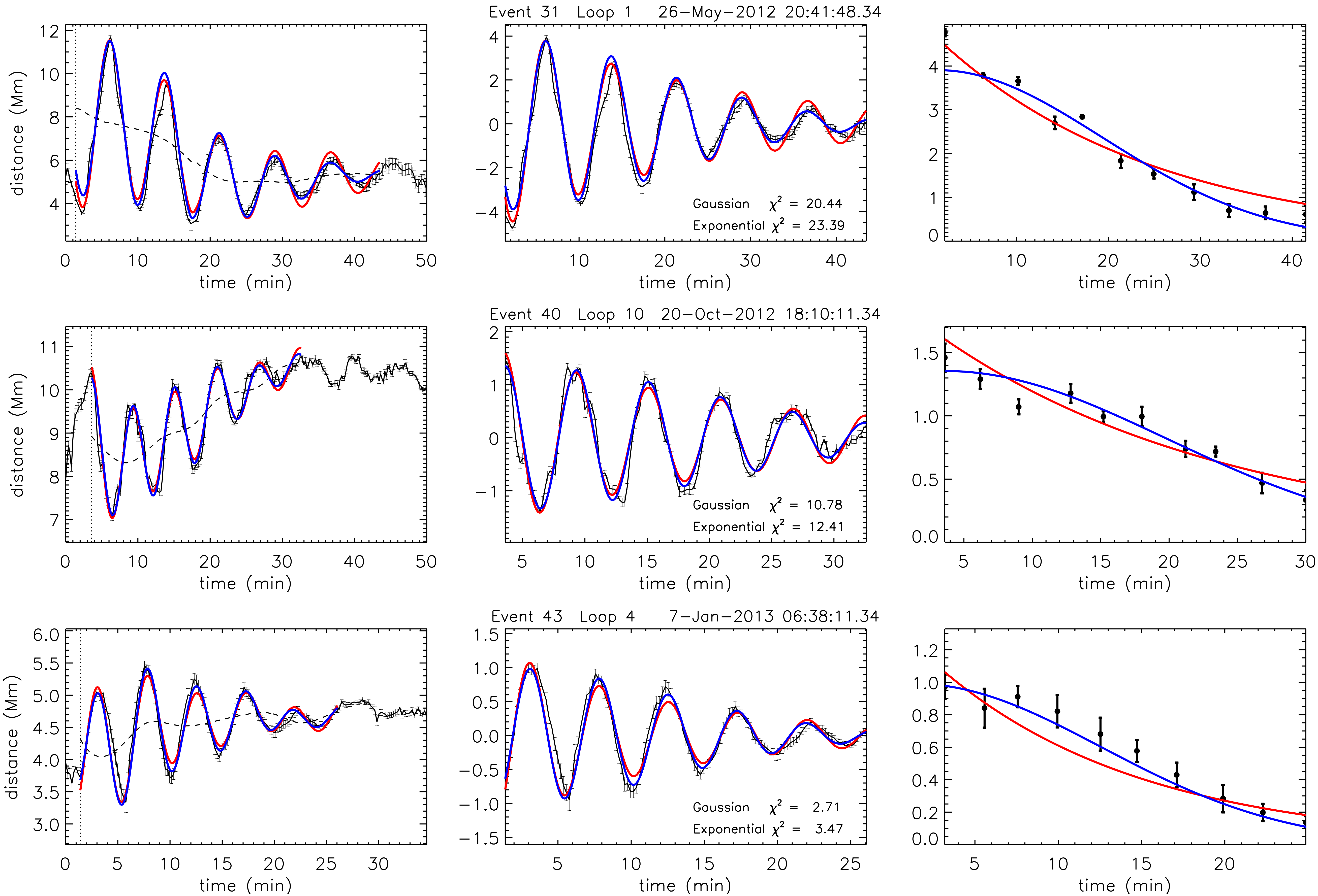

Evidence of Gaussian damping regime from SDO

- Morton & Mooroogen (2016, A&A, in press) — statistical analysis of one of the previous loops supports Gaussian damping profile

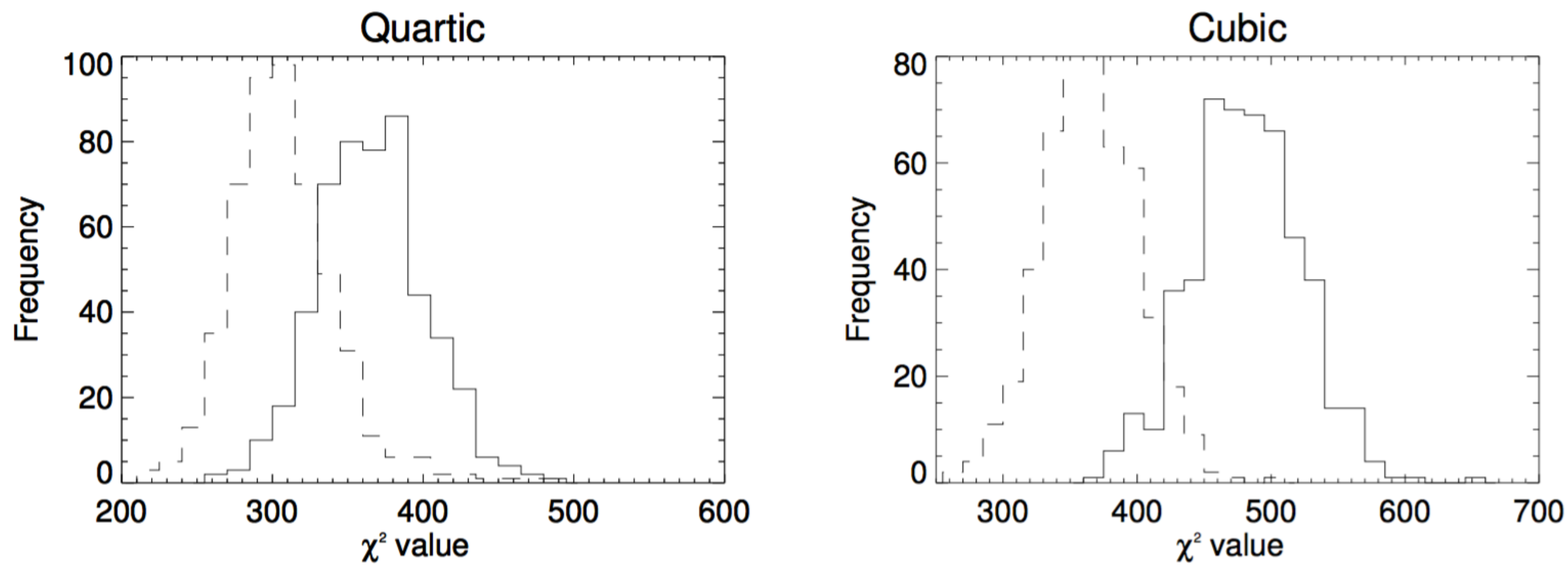

Fig. 3. Distribution of the χ^2 statistic for the quartic and cubic models. The solid lines show the distribution for the exponential damping, while the dashed line shows the distribution for the Gaussian damping.

- Model comparison:
  - Kolmogorov—Smirnoff test (Morton & Mooroogen 2016)
  - Bayesian inference (e.g. Arregui et al. 2013, ApJ, 765, L23)

Approximate damping envelope for seismology

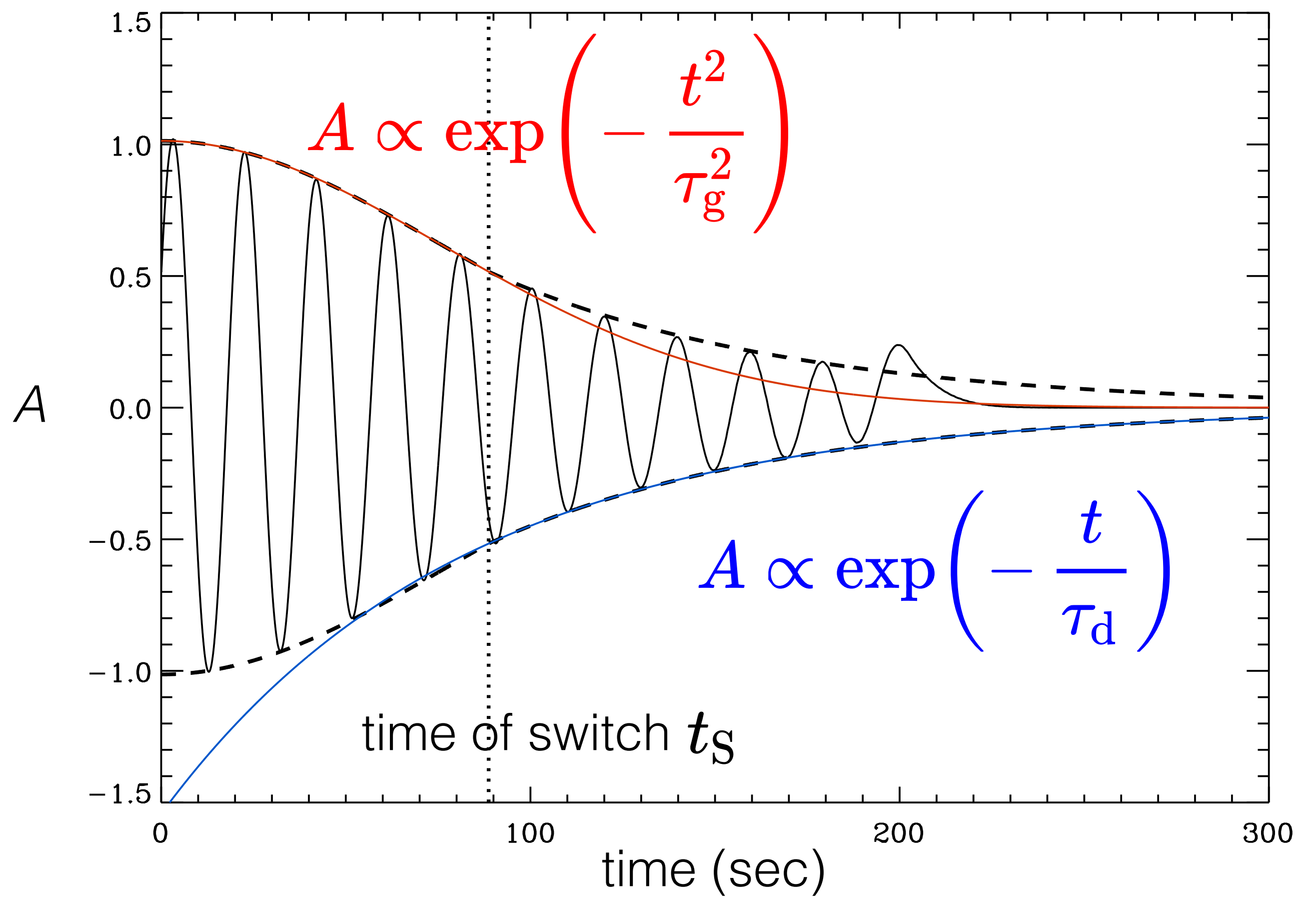

Numerical simulation of a kink mode showing **both** Gaussian and exponential damping regimes

$$t_s = \tau_g^2 / \tau_d$$

- Time of switch depends on density contrast ratio:
  - small density contrast (~2) ➝ slow switch ➝ mostly Gaussian envelope
  - large density contrast (~10) ➝ quick switch ➝ mostly exponential envelope
- If we detect both envelopes we have **two damping times** (well-posed inversion problem) ➝ unique solution for density contrast ratio and transition layer width

Hood et al. (2013)
Pascoe et al. (2013)

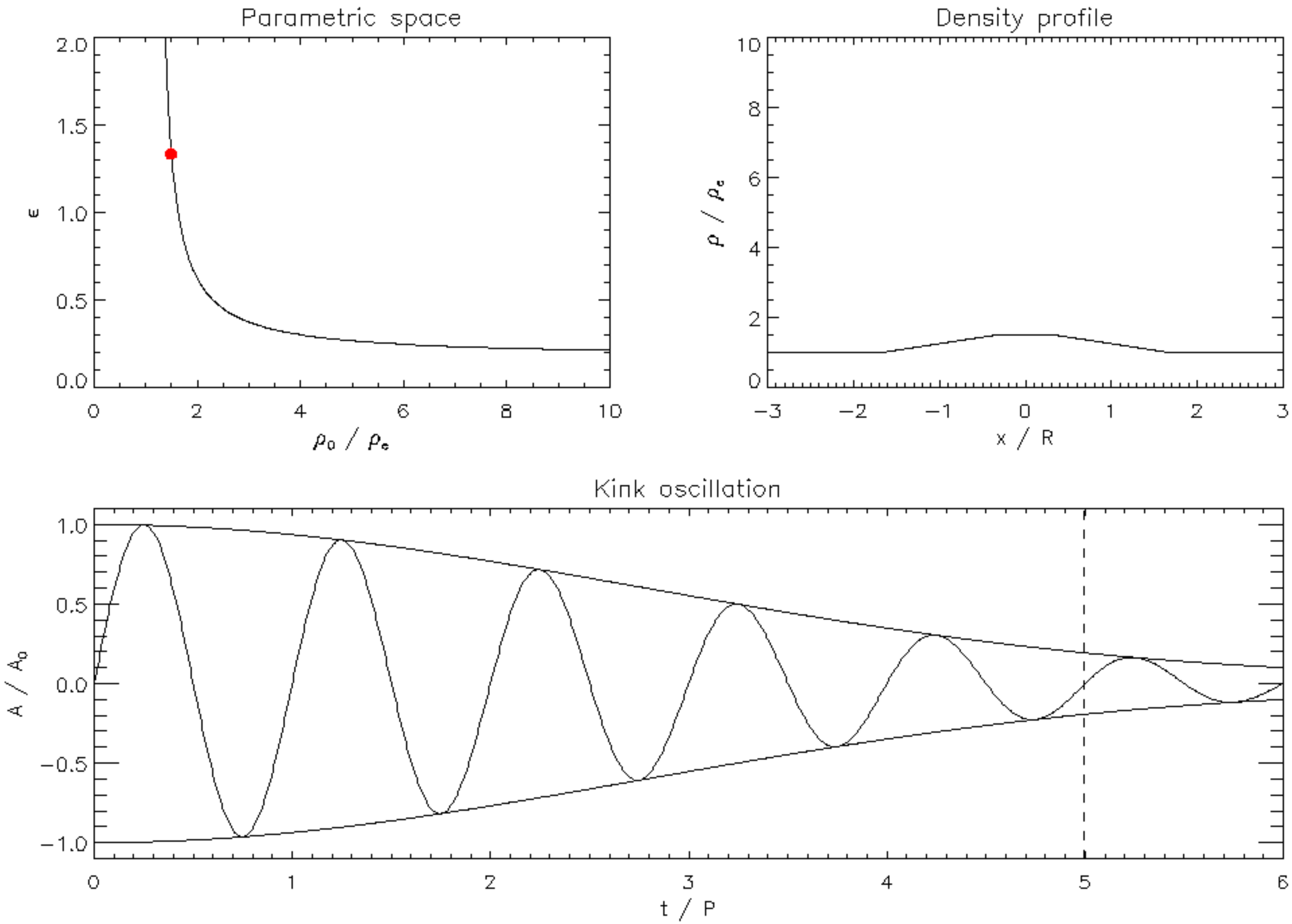

Animation shows some of the transverse loop profiles which give the same damping rate (of 90% attenuation after 6*P*)

For each structure the **shape** of the kink mode damping envelope is different

- New method uses shape of damping envelope as well as damping rate to obtain structure information

- Envelope shape is characterised by the switch time between Gaussian and exponential damping regimes:

$$t_{\rm s} = \tau_{\rm g}^2 / \tau_{\rm d}$$

General damping envelope fit to SDO data

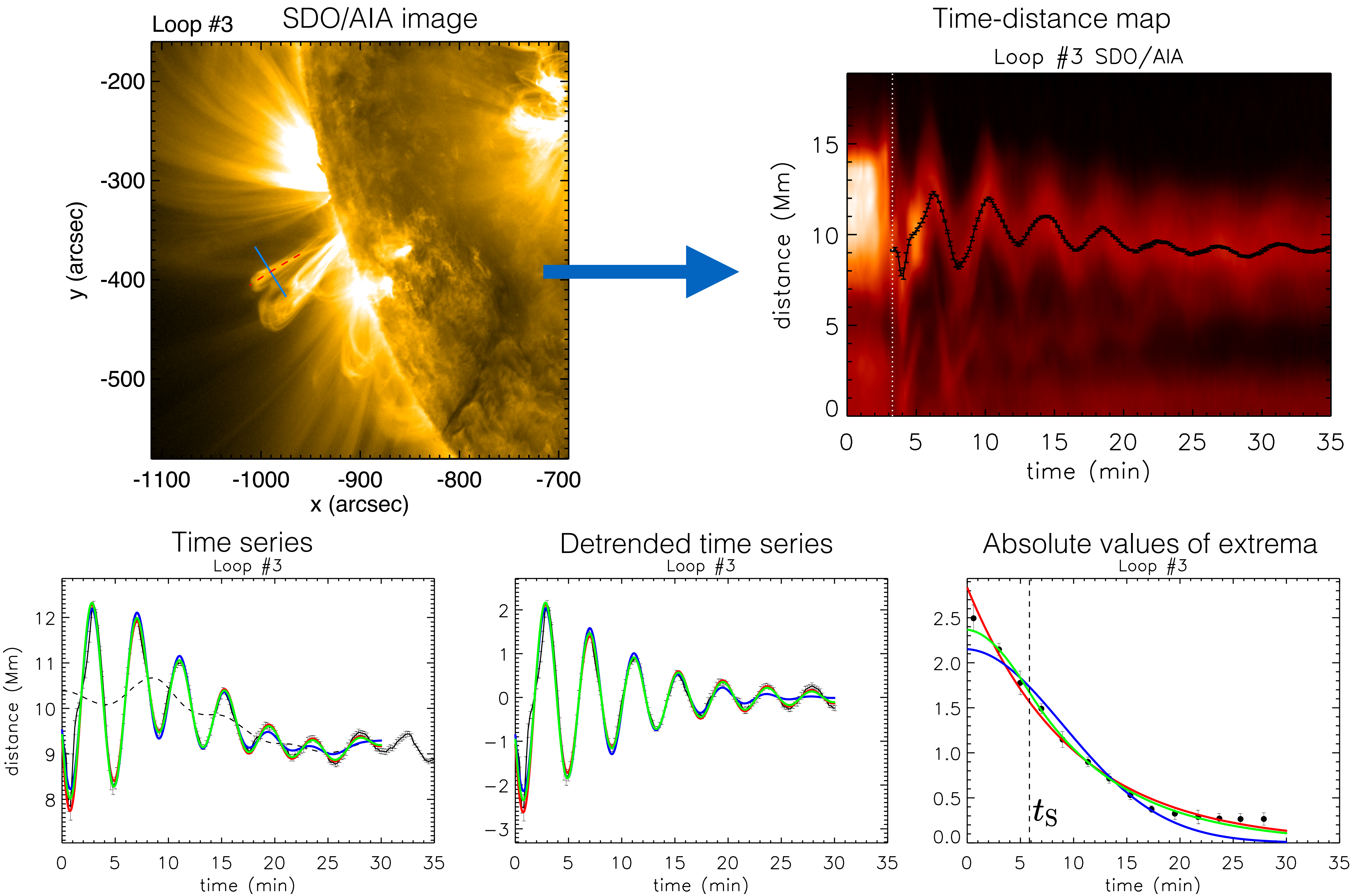

Pascoe et al. (2016, A&A, 589, A136)

General damping envelope fit to SDO data

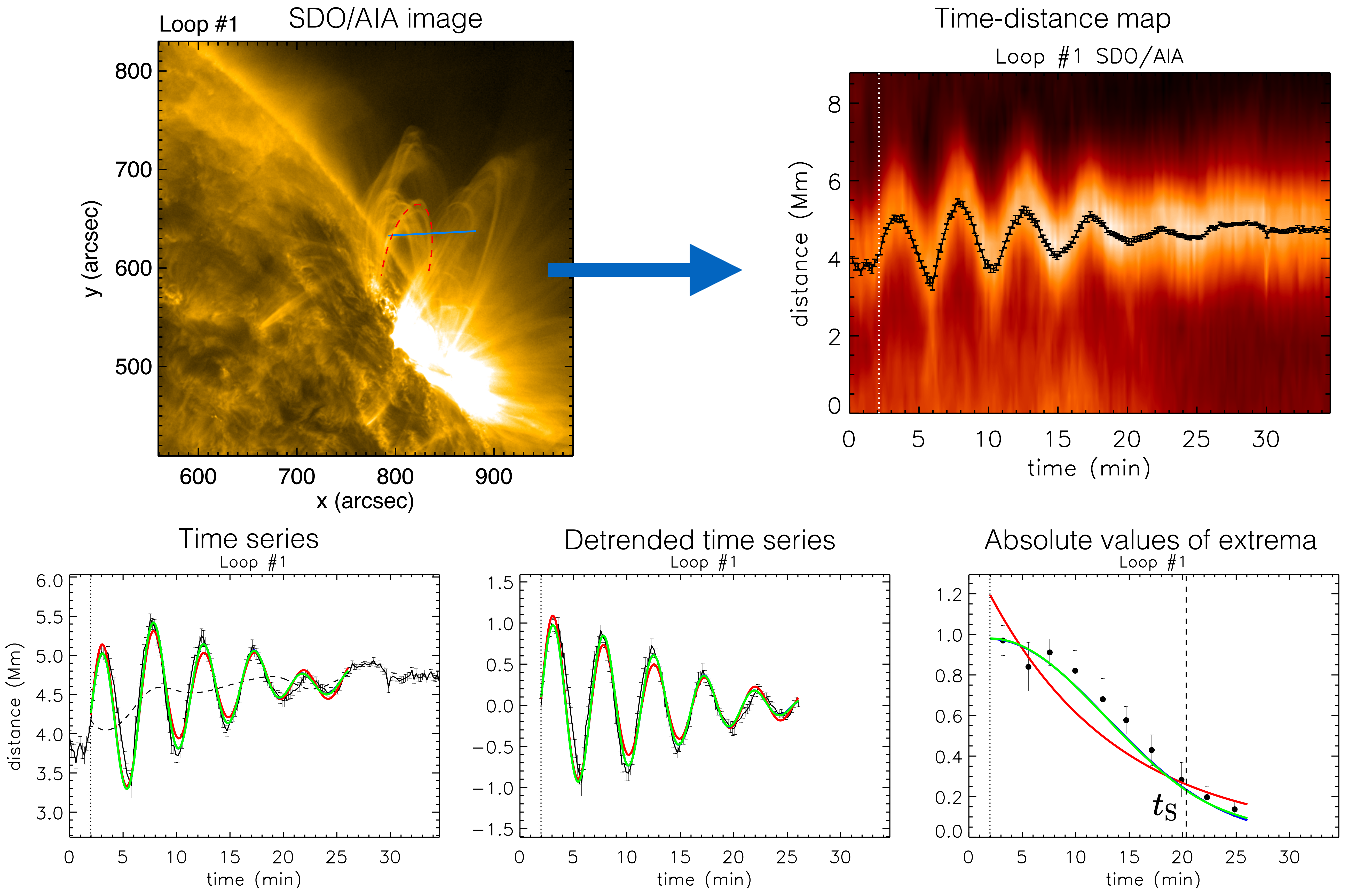

Pascoe et al. (2016, A&A, 589, A136)

Seismology of coronal loop transverse structure

- Two damping regimes (Gaussian and exponential) used to calculate the transverse loop structure

- Three loops from catalogue of Goddard et al. (2016) analysed in detail:

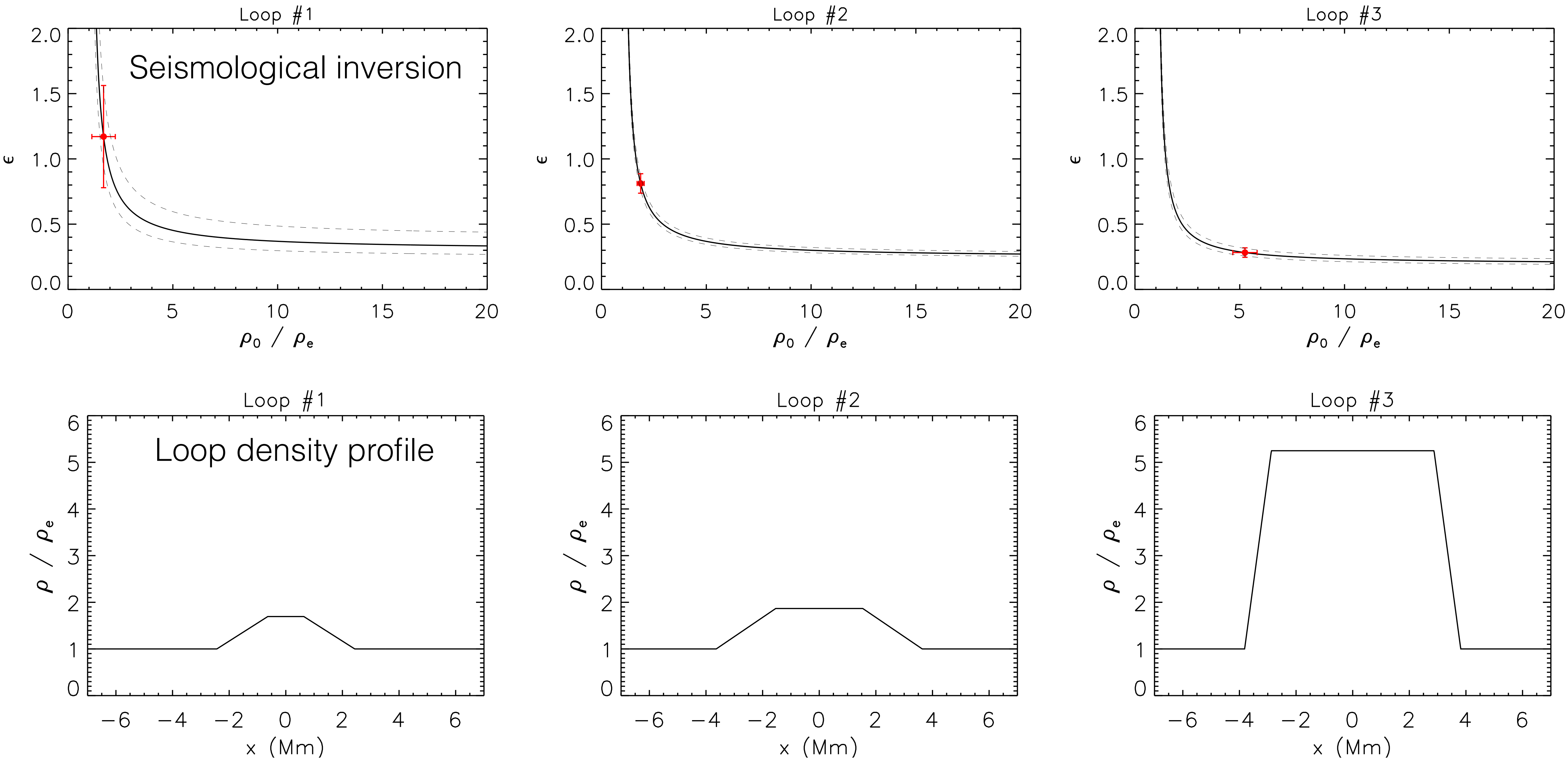

Pascoe et al. (2016, A&A, 589, A136)

Forward modelling intensity profile

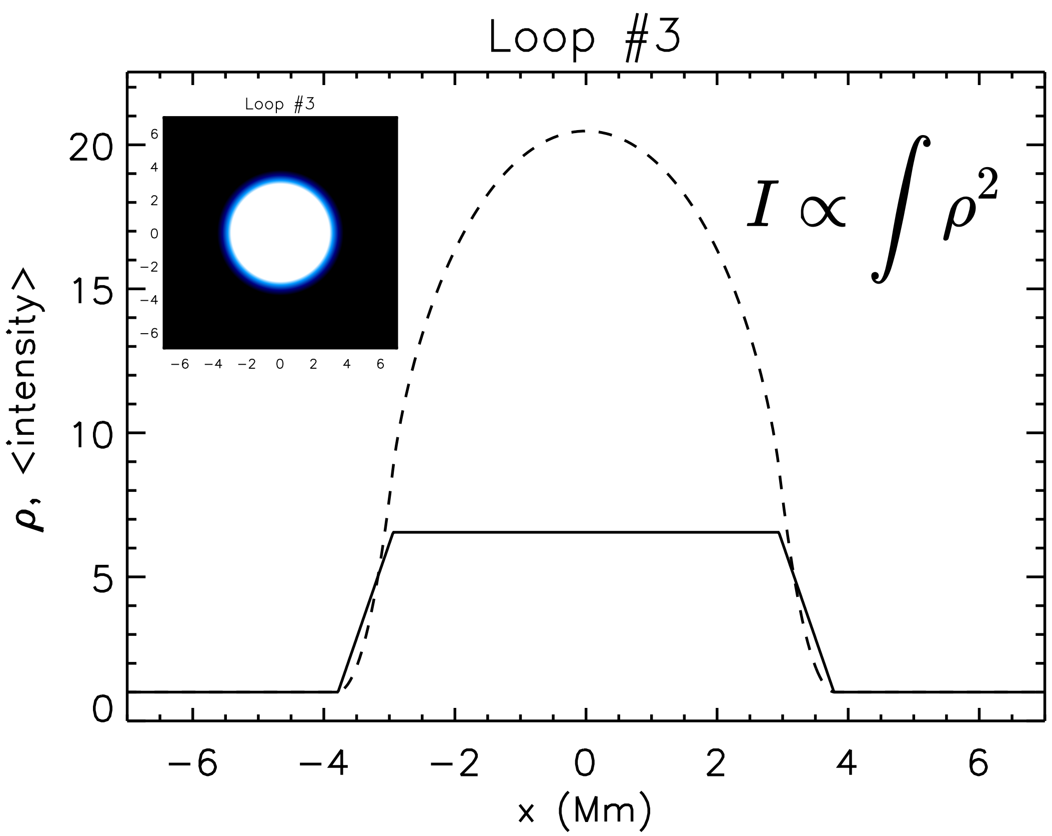

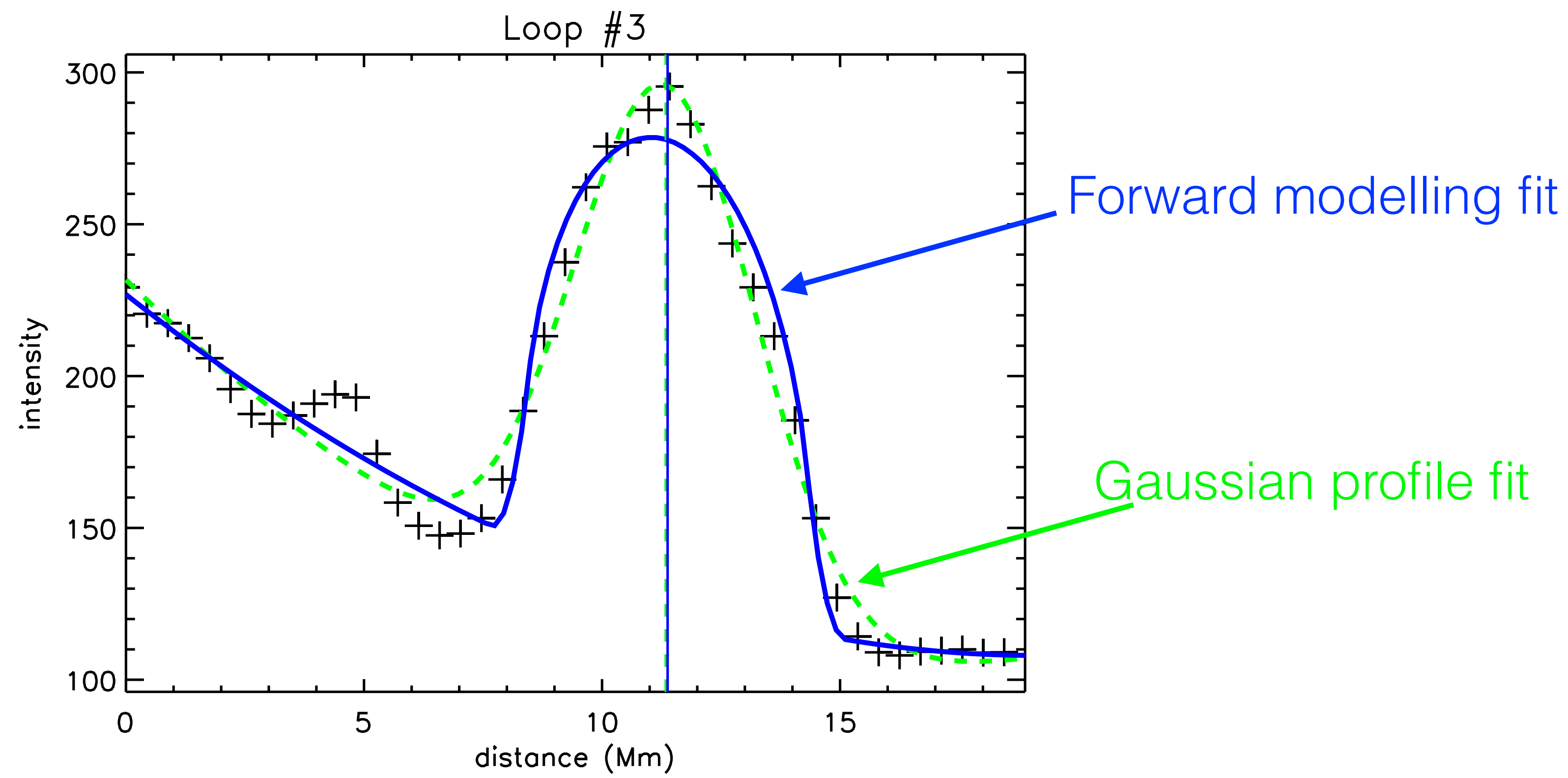

- Damping profile seismology gives $\epsilon = \dfrac{l}{R}$
- Forward modelling intensity profile and fitting to data gives *l* and *R* separately
- This method ensures same definition of *l* and *R* used in forward modelling as damping model

Pascoe et al. (2016, A&A, 589, A136)

Forward modelling TD maps

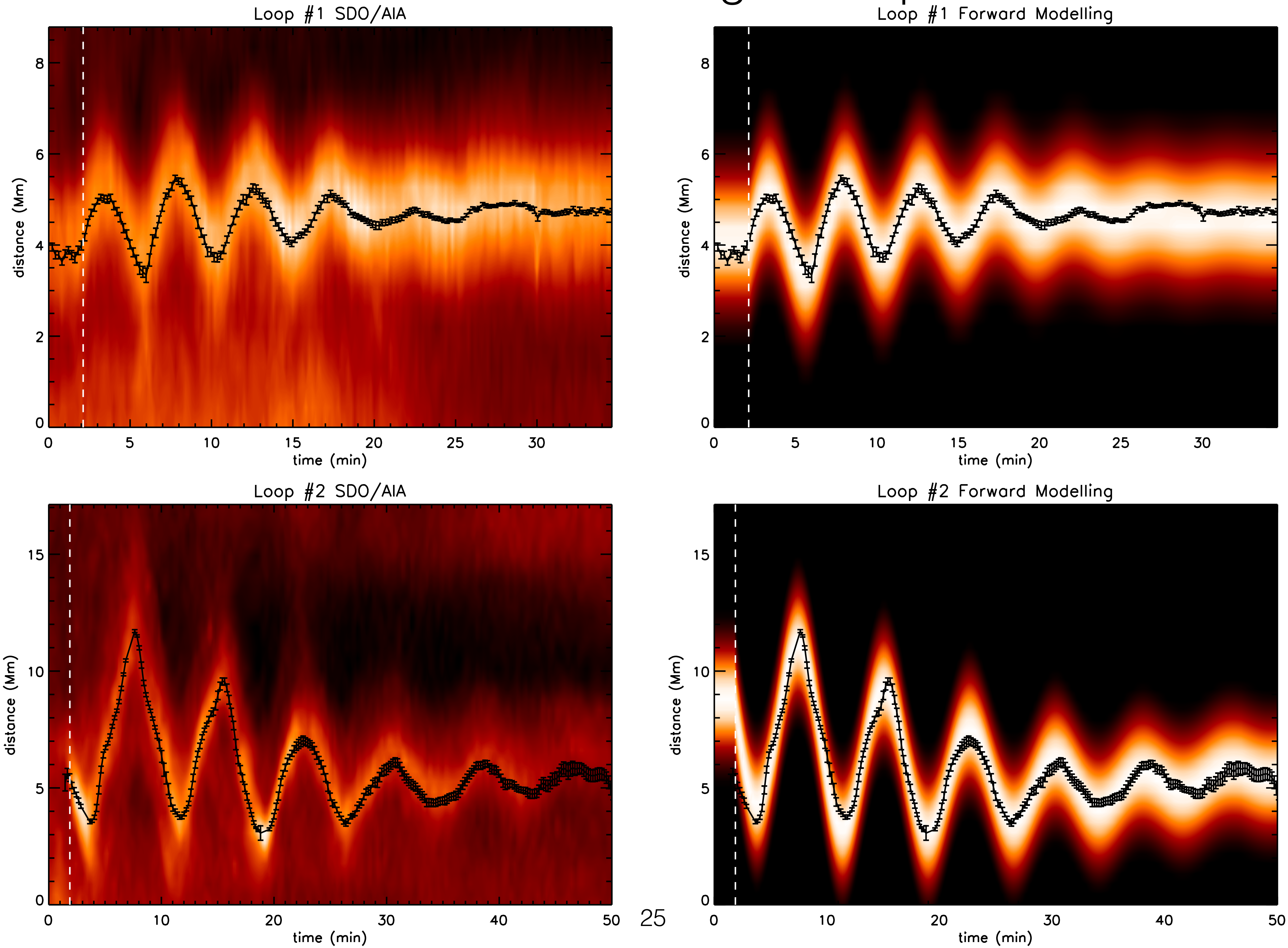

General spatial damping profile seismology

- Improved estimates of Alfvén speed by calculating actual density contrast ratio:

$$C_\mathrm{k} = 2L/P$$

$$C_\mathrm{A0} = C_\mathrm{k}/\sqrt{2/(1+\rho_\mathrm{e}/\rho_0)}$$

$$C_\mathrm{Ae} = C_\mathrm{A0}\sqrt{\rho_0/\rho_\mathrm{e}}$$

$$B_0 = C_\mathrm{A0}\sqrt{\mu_0\rho_0} = C_\mathrm{A0}\sqrt{\mu_0\bar{\mu}m_\mathrm{p}n_0}$$

$$\bar{\mu} = 1.27$$

$$m_\mathrm{p} = 1.6726\times10^{-27}\mathrm{kg}$$

$$n_\mathrm{e} = 10^{15}\mathrm{m}^{-3}$$

Loop no.	A (Mm)	ϕ (rad)	P (min)	τ_g (min)	τ_d (min)	t_s (min)	c_0	c_1	c_2
Loop #1	0.98 ± 0.02	0.10 ± 0.03	4.73 ± 0.01	10.79 ± 0.27	6.35 ± 1.50	18.32 ± 4.27	4.05	0.075	−0.0022
Loop #2	-3.97 ± 0.02	0.00 ± 0.01	7.64 ± 0.01	18.49 ± 0.15	11.24 ± 1.07	30.40 ± 2.88	9.04	−0.237	0.0035
Loop #3	-2.36 ± 0.03	0.00 ± 0.01	4.18 ± 0.00	7.24 ± 0.27	9.21 ± 0.93	5.69 ± 0.49	10.69	−0.079	0.0009

Loop no.	ρ_0/ρ_e	ϵ	R (Mm)	l (Mm)	C_k (Mm/s)	C_A0 (Mm/s)	C_Ae (Mm/s)	B_0 (G)
Loop #1	1.70 ± 0.56	1.17 ± 0.39	1.53 ± 0.13	1.79 ± 0.61	1.56 ± 0.22	1.40 ± 0.38	1.82 ± 0.65	9.39 ± 3.36
Loop #2	1.67 ± 0.22	1.10 ± 0.15	2.44 ± 0.45	2.67 ± 0.61	0.71 ± 0.14	0.63 ± 0.13	0.82 ± 0.19	4.22 ± 0.99
Loop #3	6.55 ± 0.80	0.25 ± 0.03	3.36 ± 0.28	0.84 ± 0.13	1.87 ± 0.25	1.42 ± 0.22	3.62 ± 0.65	18.72 ± 3.38

Pascoe et al. (2016, A&A, 589, A136)

Phase mixing

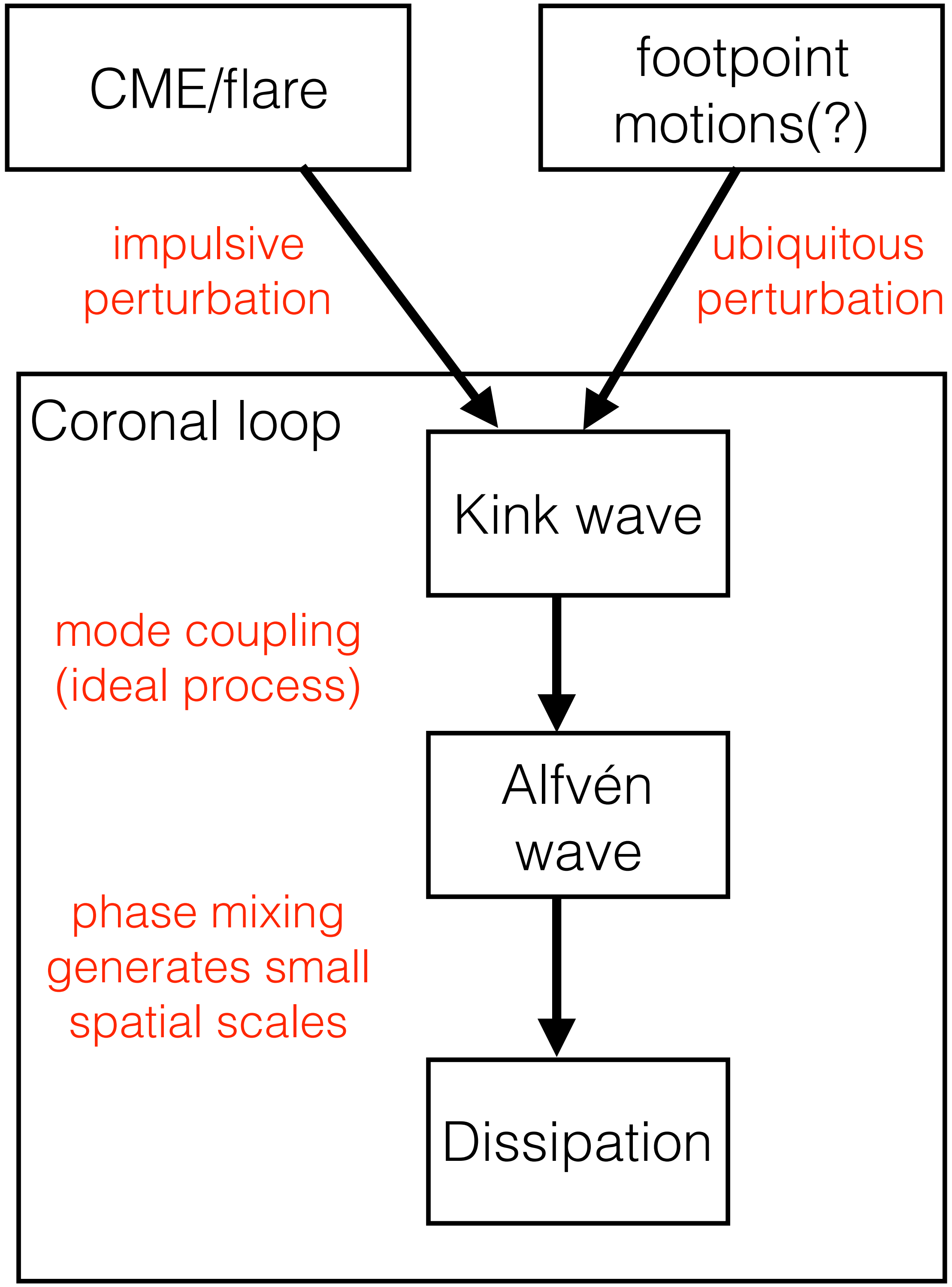

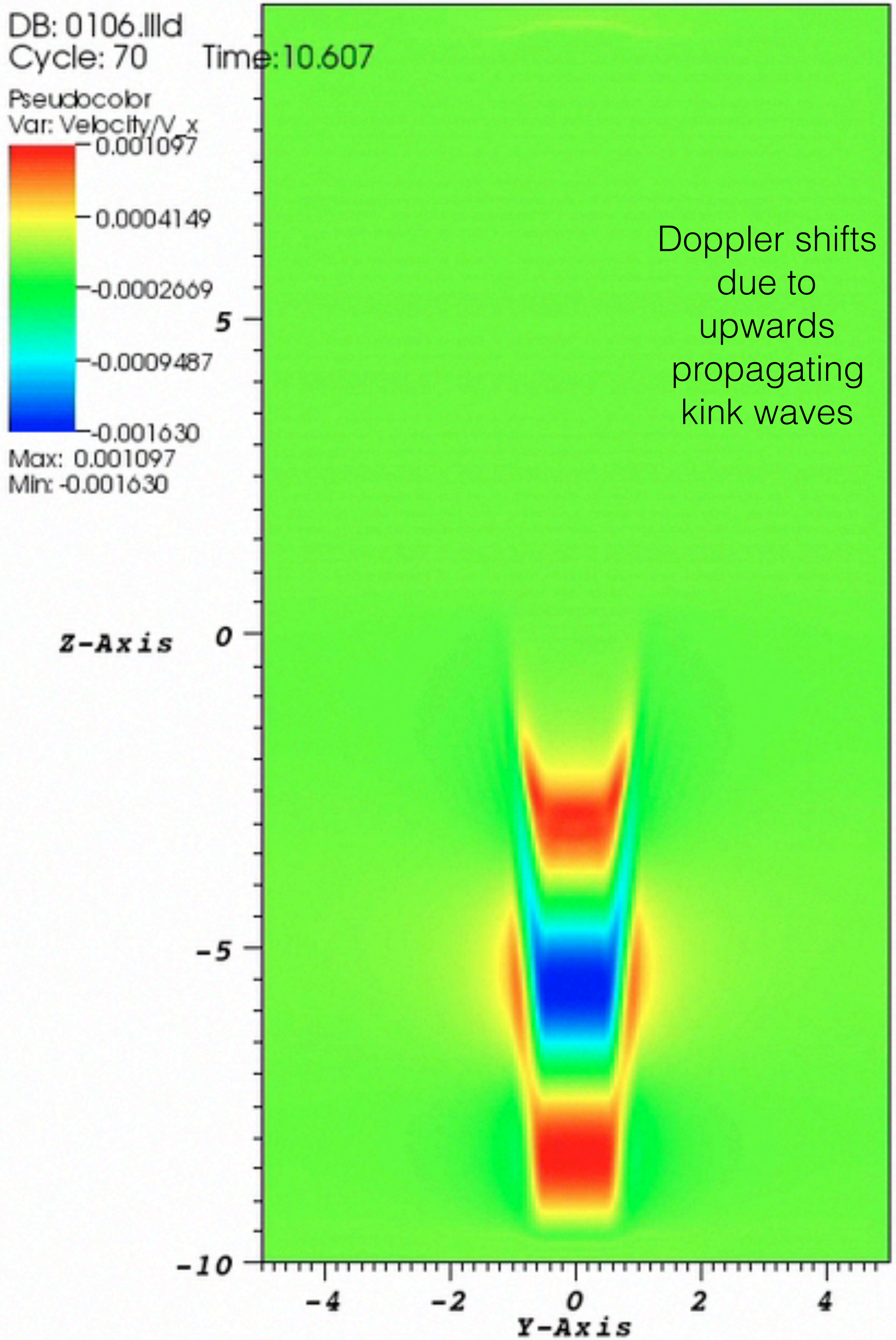

Phase mixing

- Alfvén wave generated inside inhomogeneous medium with continuous variation in local Alfvén speed — large gradients generated (e.g. Heyvaerts & Priest 1983; Cally 1991; Hood et al. 2005; Soler & Terradas 2015)

- Seismological method for determining density profile allows us to estimate phase mixing timescale

- Simulations: Mann et al. (1995):

$$L_{\rm ph} = \frac{2\pi}{\omega'_{\rm A} t}$$

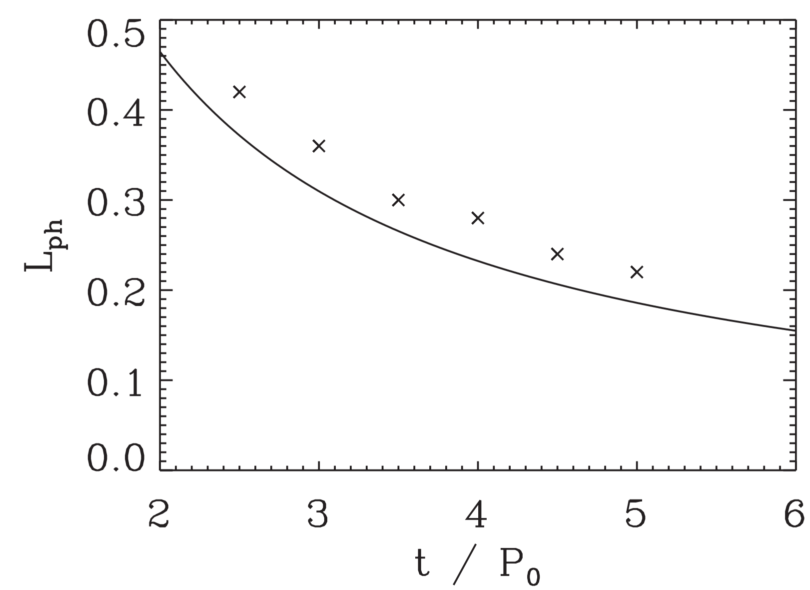

Pascoe et al. (2010)

- Observations: Based on Mann & Wright (1995):

$$\tau_{\rm A} = \frac{\epsilon L}{\pi (C_{\rm Ae} - C_{\rm A0})} \lesssim 200 \text{ seconds}$$

Pascoe et al. (2016)

Heating

- See next talk by Paolo Pagano for more details of heating
    - simulations including effects of resistivity, thermal conduction, radiative losses
- Cargill et al. (2016, ApJ, 823, 31) — wave damping creates fine structure

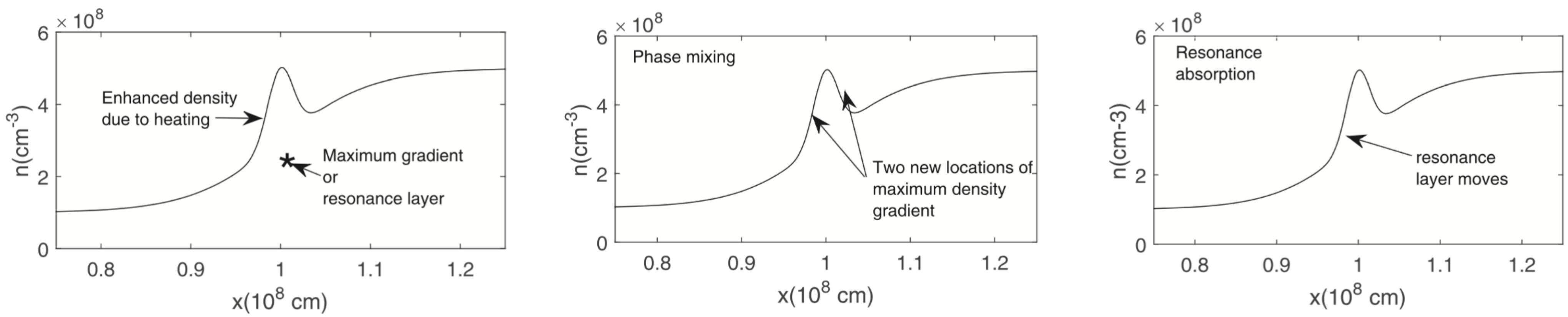

- Magyar & Van Doorsselaere (2016, ApJ, 823, 82) — waves destroy fine structure

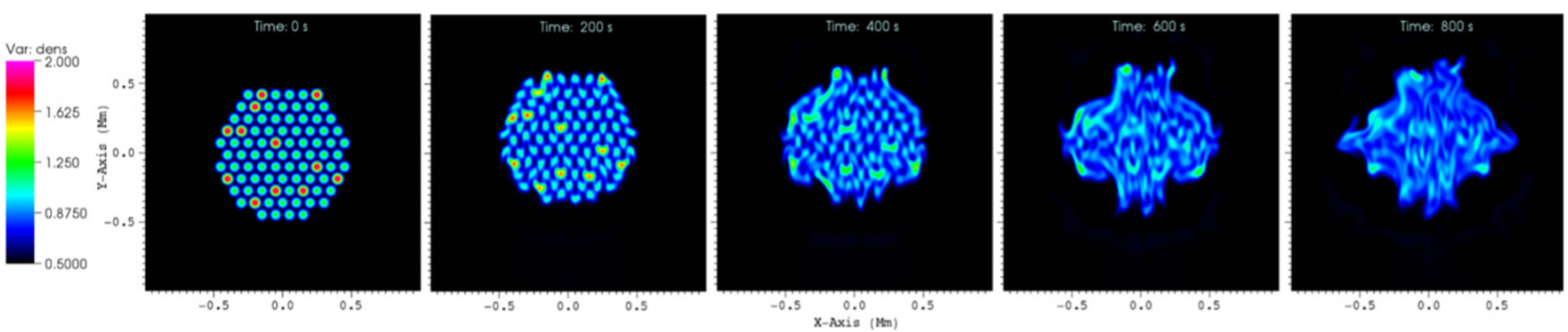

Figure 2. Plots of the loop cross-section density, at different times as indicated at the top of each panel. The slices are made at $z = 40$ Mm. The color bar is common for the plots, in units of 10^{-12} kg m^{-3}.

- (Mode coupling does not require symmetrical loops e.g. Terradas et al. 2008; Pascoe et al. 2011)

Second harmonic standing kink mode

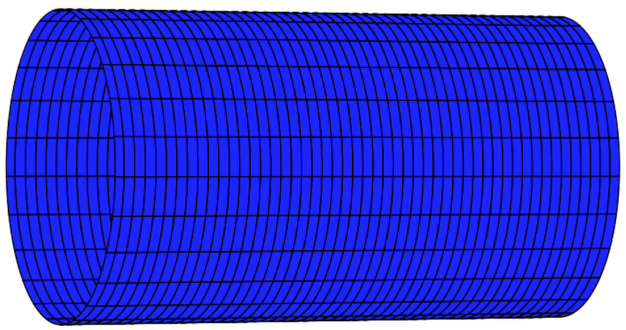

Fundamental kink mode

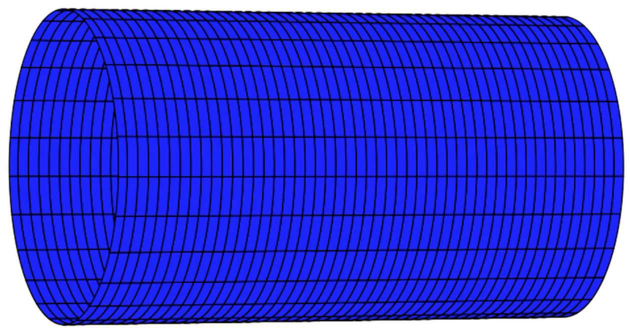

Second harmonic

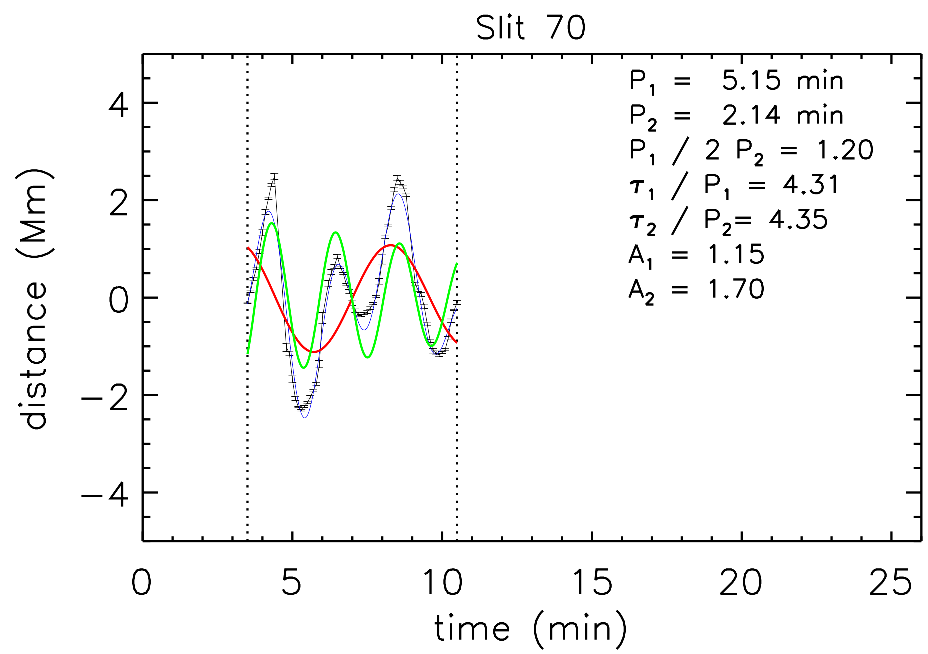

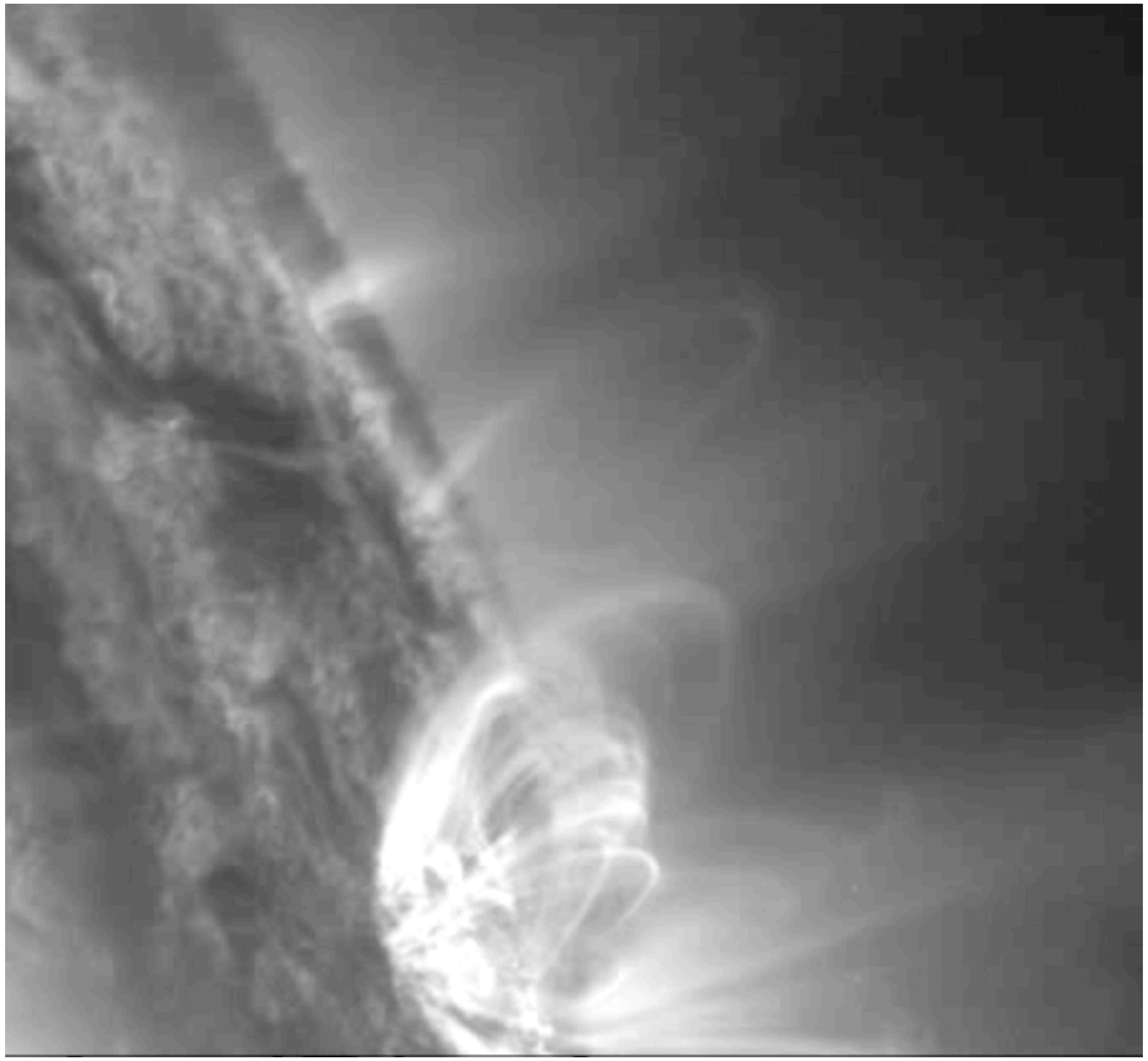

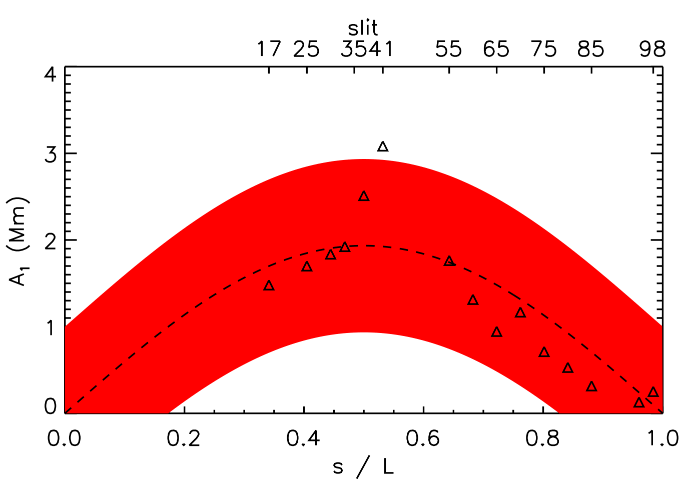

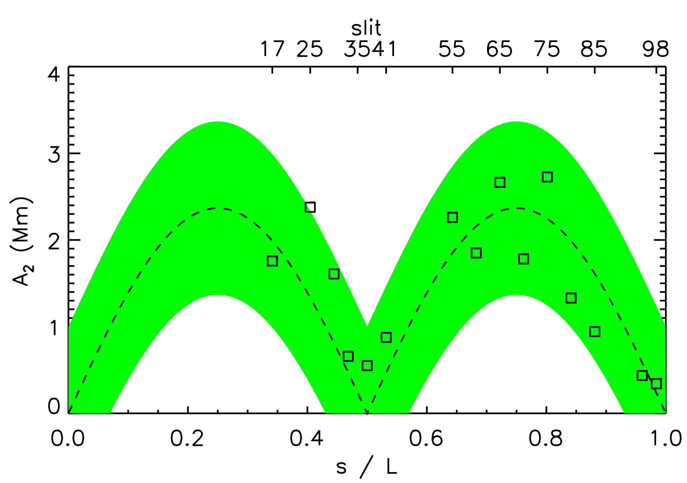

$$P_1/2P_2 = 1.15 \pm 0.22$$

Anti-phase motions of loop legs due to second harmonic

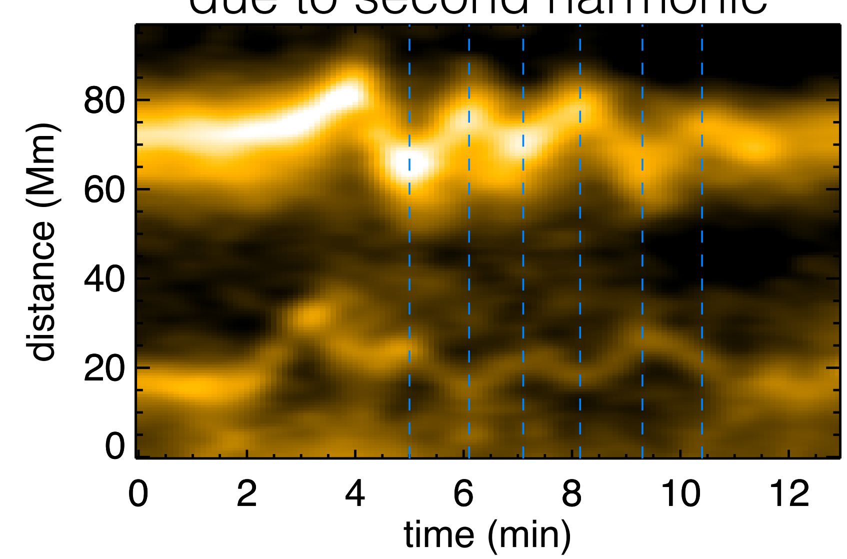

Pascoe et al. (2016, A&A, in press)

Seismology of longitudinal structuring using period ratios

- Standing kink modes usually in long wavelength limit (dispersionless) but…
- Effect of density stratification (e.g. Andries et al. 2005; Safari et al. 2007; McEwan et al. 2008)

$$\rho \propto \exp\left(-L/\pi H \sin \pi z/L\right)$$

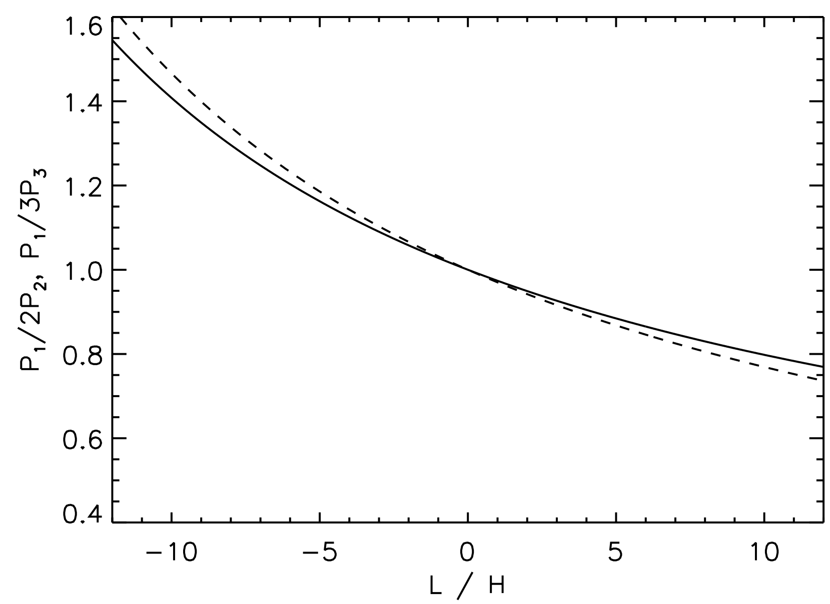

- Effect of Loop expansion (Verth & Erdélyi 2008, A&A, 486, 1015)

$$\Gamma = \frac{r_{\mathrm{apex}}}{r_{\mathrm{foot}}}$$

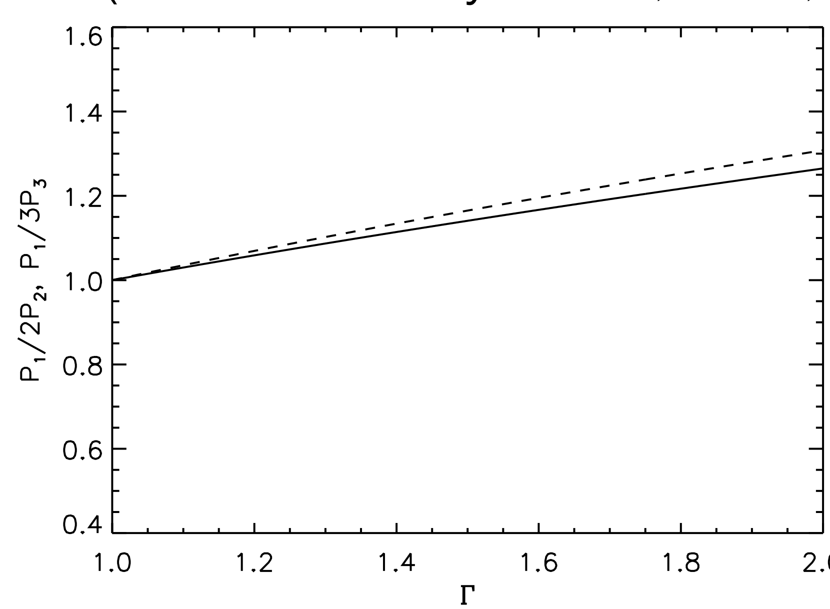

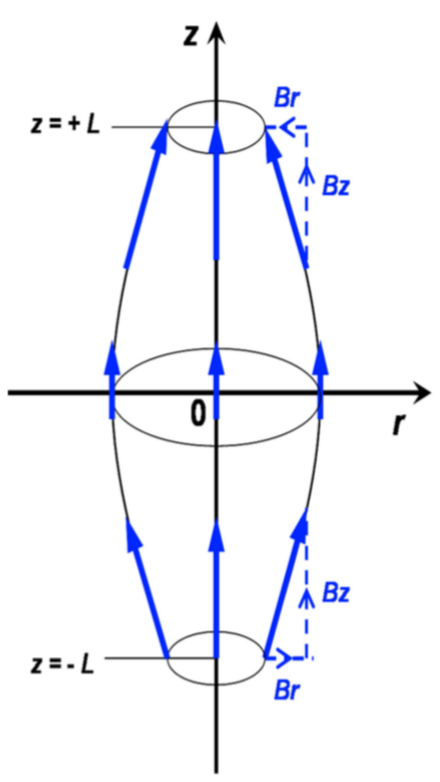

- Compare models using Bayes factors (e.g. Arregui et al. 2013, ApJ, 765, L23)

Summary

- Kink oscillations of coronal loops are damped by coupling of energy to Alfvén waves

- Numerical simulations and analytical theory predict:
  - Gaussian damping envelope for low density contrast loops
  - Exponential damping envelope for high density contrast loops

- Evidence of Gaussian damping regime recently discovered in SDO/AIA data

- Observation of both damping envelopes has allowed the transverse loop structure to be seismologically calculated for the first time

- Transverse structure essential for understanding corona e.g. improved estimates of magnetic field strength, heating rate based on phase mixing